



universität  
wien

# DIPLOMARBEIT / DIPLOMA THESIS

Titel der Diplomarbeit / Title of the Diploma Thesis

„Characterization of anti-inflammatory and anti-ageing  
activities of

*Pterocarpus santalinus*“

verfasst von / submitted by

Alexandra Pulsinger

angestrebter akademischer Grad / in partial fulfilment of the requirements for the degree of  
Magistra der Pharmazie (Mag.pharm.)

Wien, 2022 / Vienna, 2022

Studienkennzahl lt. Studienblatt /  
degree programme code as it appears on  
the student record sheet:

UA 449

Studienrichtung lt. Studienblatt /  
degree programme as it appears on  
the student record sheet:

Diplomstudium Pharmazie

Betreut von / Supervisor:

Univ.-Prof. Dr. Judith M. Rollinger



## Table of Contents

<b>1. Abstract .....</b>	<b>7</b>
<b>2. Zusammenfassung .....</b>	<b>9</b>
<b>3. Aim of the work .....</b>	<b>11</b>
<b>4. Introduction.....</b>	<b>12</b>
4.1 <i>Pterocarpus santalinus</i> .....	12
4.1.1. Characterization and botanical description of <i>P. santalinus</i> .....	12
4.1.2 Traditional use of <i>P. santalinus</i> .....	13
4.1.3. Bioactivity and Phytochemistry of <i>P. santalinus</i> .....	13
4.2 Inflammation and inflammatory diseases .....	15
4.2.1 Acute Inflammation .....	15
4.2.2. Chronic inflammation .....	16
4.2.3 NF $\kappa$ B signaling pathway .....	16
4.2.4 HSPA1A and its role in oxi-inflamm-aging .....	18
4.3. Cell culture as an <i>in vitro</i> study model .....	18
4.3.1 HUVEC primary cells.....	18
4.3.2. HEK-293 cells.....	20
<b>5.Results and Discussion .....</b>	<b>21</b>
5.1 Pharmacological investigation of <i>Pterocarpus santalinus</i> in HUVEC cells .....	21
5.1.1 Dose response study with TNF and LPS .....	21
5.2. Pharmacological investigation of <i>Pterocarpus santalinus</i> in HEK-293 cells .....	36
5.2.1 Cell viability assay for PS in HEK-293 cells .....	36
5.2.2 Dose response study of PS in HEK 293 cells.....	37
5.2.3 Kinetic analysis of HSPA1A expression in HEK-293 cells.....	39
5.2.4 Real time PCR analysis for microfractions 1-35 .....	40
<b>6. Conclusion .....</b>	<b>42</b>
<b>7. Materials and Methods .....</b>	<b>44</b>
7.1 Preparation of <i>P. santalinus</i> extract and fractions .....	44
7.2 Cell culture-HUVEC .....	44
7.2.1 HUVEC isolation from umbilical cords .....	44

7.2.2 HUVEC passaging .....	46
7.2.3 Real-time PCR analysis .....	46
7.3 Cell-culture HEK-293 cell-line .....	51
7.3.1 Thawing of HEK-293 cells .....	51
7.3.2 HEK-293 passaging .....	51
7.3.3 Freezing of HEK-293 cells .....	52
7.3.4 Cell Titer-Blue Cell Viability assay .....	52
7.3.5 Real-time PCR analysis in HEK-293 cells .....	54
7.4 Instruments and Products .....	55
<b>8. Acknowledgments.....</b>	<b>56</b>
<b>9. References .....</b>	<b>57</b>

## List of abbreviations

AGE	Advanced Glycation End Product
ATCC	American Type Culture Collection
ATP	Adenosine Triphosphate
BHLH	Basic Helix Loop Helix Transcription Factor
CD8	Cluster of Differentiation 8
CD4	Cluster of Differentiation 4
cDNA	Complementary Deoxyribonucleic acid
CFP	Chloroform Bioactive Fraction of <i>P. santalinus</i>
CX3CL1	C-X3-C Motif Ligand 1
DEPC	Deionized, Diethylpyrocarbonate
DMEM	Dulbecco's Modified Eagle's Limiting Media
DMSO	Dimethyl Sulfoxide
dNTPs	Deoxynucleotide Triphosphates
DPPH	1,1-Diphenyl-2-Picrylhydrazyl
EC	Endothelial Cell
ECGS	Endothelial Cell Growth Supplement
FBS	Fetal Bovine Serum
FCS	Fetal Calf Serum
GAPDH	Glyceraldehyde-3-Phosphate Dehydrogenase
HEK	Human Embryonic Kidney
HeLa	Henrietta Lacks
Hsp	Heat shock protein
HUVEC	Human Umbilical Vein Endothelial Cells
ICAM-1	Intercellular adhesion molecule 1
I $\kappa$ B	Inhibitor of Nuclear Factor Kappa B
IL-1	interleukin 1
IRF	Interferon regulatory factor
LPS	Lipopolysaccharide
MEK/ MAP2K	Mammalian Mitogen-Activated Protein Kinase Kinase Kinase
mRNA	Messenger Ribonucleic Acid

NF	nuclear factor
NF $\kappa$ B	Nuclear Factor of 'kappa-light-chain-enhancer' of Activated B-cells
NIK	NF- $\kappa$ B-Inducing Kinase
NO	Nitric Oxide
NSAID	Non-Steroidal Anti-Inflammatory Drug
PARP	Peroxisome-Activated Receptor Protein
PBS	Phosphate Buffered Saline
PCR	Polymerase Chain Reaction
PDGF	Platelet-Derived Growth Factor
PPAR- $\gamma$	Peroxisome Proliferator-Activated Receptor- $\gamma$
PS	<i>Pterocarpus santalinus</i>
RT	Reverse Transcriptase
SREBP-1c	Sterol Regulatory Element-Binding Protein-1c
TNF	Tumor Necrosis Factor
TRAF	TNF Receptor-Associated Factor
UV	Ultraviolet
VCAM-1	Vascular Cell Adhesion Molecule-1

## 1. Abstract

Inflammation and inflammatory reactions play a key role in several maladies including cardiovascular, neurodegenerative, gastrointestinal diseases as well as joint and skin disorders. Despite several steroidal and non-steroidal drugs currently being available for the treatment of inflammatory diseases, there are also certain limitations for their use, especially for chronic illnesses, suggesting that novel-lead structures are crucial. Natural products not only have been traditionally used for a long time as anti-inflammatory treatment but also offer a rich source for novel secondary metabolites, that interfere with key players in inflammation. One of these natural products is *Pterocarpus santalinus* L.f. (PS), also known as red sandalwood. The heartwood of *P. santalinus* is frequently used in Ayurveda for the treatment of various diseases, including inflammation and oxidative stress. Several scientific reports also confirm the anti-inflammatory potential of red sandalwood.

The first part of this diploma thesis focuses on the investigation of the anti-inflammatory activity in an *in vitro* model of tumor necrosis factor (TNF) and lipopolysaccharide (LPS) stimulated endothelial cells. Previous studies have demonstrated an inhibitory effect of PS in interleukin 1(IL-1) stimulated human umbilical vein endothelial cells (HUVEC). In order to extend these studies to further inflammatory stimuli, LPS and TNF were chosen for stimulation. PS suppressed the expression of various genes, that play a critical role in the inflammatory process. The three genes mostly effected were CX3CL-1 a chemokine, VCAM1 a cell adhesion molecule, both responsible for the recruitment of inflammatory cells at the site of inflammation, as well as TRAF1, which acts as a feedback loop for TNF and LPS signaling pathways. CX3CL1 levels were reduced by 96%, TRAF1 and VCAM-1 by 99%. Further proinflammatory genes downregulated were CSF2, PLA2 and IRF1. Oppositely, PS also induced gene expression of the nuclear hormone receptors NR4A1/2/3 as well as of the transcription factor BHLHE40 and the zinc finger protein ZFP36. All three exhibit potential negative regulatory functions. These findings suggest that PS mostly acts in an inhibitory manner against inflammatory processes but might also promote some inflammatory reactions.

The second part of this diploma thesis was dedicated to the investigation of HSPA1A expression in PS treated HEK-293 cells. In prior conducted experiments with PS in HUVEC an upregulation of HSPA1A expression was observed, independent of pro-inflammatory stimulation. As HEK-293 cells provide a simpler experimental system compared to primary

cells and simplify the analysis of a larger group of samples, they were chosen for the following experiments. A dose dependent induction for PS was determined with the highest amplification noticed at 50 µg/ml. *P. santalinus* was further fractionized and microfractions were also screened for HSPA1A expression, with a few fractions showing increased gene expression. The oxidation-inflammation theory of aging states, that the core age- related alterations of body cells are chronic oxidative stress and inflammatory stress situations. HSPA1A is released under stressful conditions and acts as a cellular defense mechanism. Based on HSPA1A showing protection against harmful effects of oxidative stress and modulating the inflammatory status, it might be an important regulator of the rate of aging. Increased levels of HSPA1A through sandalwood might be connected to its potential anti-ageing effect.



## 2. Zusammenfassung

Entzündungen und Entzündungsreaktionen spielen eine Schlüsselrolle in zahlreichen Erkrankungen, einschließlich kardiovaskulären, neurodegenerativen und gastrointestinalen sowie Gelenks- und Hautbeschwerden. Zurzeit sind einige steroidale und nicht-steroidale Arzneimittel für die Behandlung von Entzündungen erhältlich, jedoch gibt es bestimmte Einschränkungen in deren Gebrauch, besonders bei chronischen Erkrankungen. Daher ist die Forschung an neuen Leitstrukturen essenziell. Naturprodukte werden nicht nur schon seit einem langen Zeitraum traditionell bei Entzündungsbeschwerden eingesetzt, sondern sind auch reich an neuartigen Sekundärmetaboliten, die mit Schlüsselfaktoren der Entzündungsreaktionen interagieren. Eines dieser Naturprodukte ist *Pterocarpus Santalinus* L.f. (PS), umgangssprachlich als rotes Sandelholz bekannt. Das Kernholz von *P. Santalinus* wird weit verbreitet in Ayurveda für die Behandlung vielfacher Erkrankungen, einschließlich Entzündungen und oxidativem Stress angewendet. Mehrere wissenschaftliche Artikel belegen die mögliche entzündungshemmende Wirkung des Sandelholzes.

Der erste Teil dieser Diplomarbeit fokussiert sich auf die Untersuchung der entzündungshemmenden Aktivität in einem *in vitro* Model von Tumornekrose Faktor (TNF) und Lipopolysacchariden (LPS) stimulierten Endothelzellen. Zuvor durchgeführte Studien wiesen einen hemmenden Effekt von PS in mit Interleukin 1 (IL-1) stimulierten Endothelzellen, die von humanen Bauchnabelschnüren isoliert wurden, auf. Um diese Studien weiter zu vertiefen, wurden nun LPS und TNF als Stimulatoren gewählt. PS verringerte die Expression verschiedener Gene, die eine kritische Rolle während des Entzündungsprozesses spielen. Die drei Gene, die am meisten betroffen waren, waren CX3CL1, ein Chemokin, VCAM1, ein Zelladhäsion Molekül, beide verantwortlich für die Rekrutierung der Entzündungszellen zum Ort der Entzündung, sowie TRAF1. TRAF1 agiert als Rückkopplungsschleife für TNF und LPS Signalwege. CX3CL1 Level wurden um 96% reduziert, TRAF1 und VCAM-1 um 99%. Weitere herunterregulierte Gene waren CSF2, PLA2 und IRF1. Im Gegenzug induzierte das Sandelholz auch die Genexpression der nuklearen Hormonrezeptoren NR4A1/2/3 sowie der Transkriptionsfaktoren BHLHE40 und ZFP36. Diese weisen potenzielle negative Regulationsfunktionen auf. Diese Ergebnisse geben Grund zur Annahme, dass PS vor allem hemmende Wirkung gegen inflammatorische Prozesse aufweist, jedoch auch einige Entzündungsreaktionen fördert.

Der zweite Teil dieser Arbeit befasst sich mit der Untersuchung der HSPA1A Expression in mit PS behandelten HEK-293 Zellen, da zuvor durchgeführte Experimente eine erhöhte HSPA1A Expression durch PS in Endothelzellen aufwiesen. Dadurch, dass HEK-293 Zellen im Vergleich zu primären Zellen ein einfacher zu händelndes experimentelles System darstellt und die Analyse einer großen Anzahl von Proben vereinfacht, wurde dieses Modell für die folgenden Experimente gewählt. Eine dosisabhängige Induktion von PS wurde festgestellt, wobei die höchste Verstärkung bei 50 µg/ml beobachtet worden war. *P. santalinus* wurde weiter fraktioniert und die Mikrofraktionen ebenfalls auf ihre HSPA1A Expression gescreent. Einige Fraktionen wiesen eine verstärkte Genexpression auf. Zuvor durchgeführte Studien zeigten vielversprechende lebensverlängernde Ergebnisse für *P. santalinus* auf. Die Oxidations-Entzündungstheorie des Alterns besagt, dass die altersbedingten Veränderungen der Körperzellen hauptsächlich auf chronisch oxidativen Stress und inflammatorischen Stresssituationen bedingt sind. HSPA1A wird unter stressvollen Konditionen freigesetzt und agiert als zellulärer Abwehrmechanismus. Darauf basierend, dass HSPA1A Schutz gegen die schädlichen Effekte des oxidativen Stresses bietet und den Entzündungsstatus moduliert, könnte es ein wichtiger Regulator im Alterungsprozess darstellen. Erhöhte HSPA1A Levels aufgrund von Sandelholz könnten einen Einfluss auf den potenziellen Anti-Aging Effekt haben.

### 3. Aim of the work

*P. santalinus* has traditionally been used for a long period of time for the treatment of various diseases including oxidative stress and inflammation. Various scientific reports have been published demonstrating the potential anti-inflammatory and anti-ageing effect of sandalwood. The aim of this diploma thesis is to further investigate these effects by focusing on its pharmacological activities. The thesis can be split in two parts.

The first part analyzes the anti-inflammatory activity using real time PCR analysis. This was conducted through stimulation of endothelial cells with various stimuli and examination of downregulated or upregulated genes, that play a critical role in the inflammatory process. Endothelial cells were chosen as the *in vitro* study model due to their importance during inflammatory reactions.

For the second part of the thesis real time PCR analysis with HSPA1A as the primer were performed and HEK-293 cells were used as the *in vitro* study model. HEK-293 cells were treated with PS and microfractions of PS. The aim was to establish and evaluate an alternative assay system, as HEK-293 cells provide a simpler experimental system compared to primary cells and thus simplify the analysis of a large group of samples, such as microfractions. Previous performed experiments showed an amplification of HSPA1A levels through PS treatment in HUVEC. Studies have linked enhanced HSPA1A levels with longevity. Thus, higher levels could be linked to the potential anti-ageing effect of sandalwood.

## 4. Introduction

### 4.1 *Pterocarpus santalinus*

#### 4.1.1. Characterization and botanical description of *P. santalinus*

*Pterocarpus santalinus* L.F. (*P. santalinus*) also commonly known as red sandalwood or red sanders belongs to the family of Fabaceae and is primary located in southern India (Shou-Fang et al. 2011). It is a small to medium sized deciduous tree with a blackish brown bark, 1-1,5 cm thick (Kankanange et al. 2011). The heartwood of red sanders is based on its name, red-colored, owing to the presence of the natural dye santalin and also very hard. Due to its red elegant wood, it is widely commercially used for handicrafts, furniture making and carving but it also has a great medicinal value (Dahat et al. 2021). The leaves of *P. santalinus* are 3 foliated, 10-18 cm long with usually 3 leaflets, that are egg-shaped or orbicular. Flowers are yellow, about 2 cm, bisexual, fragrant and stalked in short racemes (Kankanange et al. 2011).



Figure 1 *Pterocarpus santalinus* tree



Figure 2 Heartwood of *P. santalinus*

<sup>1</sup>[sailasyahitechnursery.com/red\\_sandalwood](http://sailasyahitechnursery.com/red_sandalwood)

<sup>2</sup>[indiasendangered.com/red-alert-for-red-sanders-the-rare-red-coloured-timber](http://indiasendangered.com/red-alert-for-red-sanders-the-rare-red-coloured-timber)

#### 4.1.2 Traditional use of *P. santalinus*

*P. santalinus* is a valuable medical plant, which is frequently used in Ayurveda, an Indian system of traditional medicine. Therefore, the heartwood of *P. santalinus* is used externally for the treatment of e.g., inflammation, diabetes, for skin diseases, jaundice, headaches as well as in wound healing (Bulle et al. 2016). In many traditional/ayurvedic formulations it also plays an important role for the treatment of various diseases. Pushyanuga Churna, a polyherbic formulation, that is indicated for female reproductive disorders or Mudgha Lepa, a herbo-mineral formulation, that is used as an anti-acne treatment are two examples for these well-acknowledged formulations. Bath soaps made out of *P. santalinus*, as well as wood powder, which is applied as a paste, can also be found in local markets for skin disorders (Dahat et al. 2021). The wood of *P. santalinus* is also widely used in the manufacturing of furniture, musical instruments, dye, and cosmetics (Kankanange et al. 2011).

#### 4.1.3. Bioactivity and Phytochemistry of *P. santalinus*

Through a number of phytochemical studies around the globe, researchers were able to identify various classes of chemical constituents of *P. santalinus*. Sesquiterpenes and polyphenolics are primarily present in the heartwood, while triterpenoids can mainly be found in the leaves and bark of the plant. Phytochemicals, that were already identified are sesquiterpenes, triterpenes, steroids, flavonoids, benzofurans, coumarins, lignans, pterocarpan, auron glycosides, chalcones, hydroxybenzoic acids, miscellaneous (several constituents belonging to various classes such as stilbenes) as well as pigments (Santalin A, B and Y) (Dahat et al. 2021; Bulle et al. 2016).

Many *in vitro* and *in vivo* studies have confirmed that molecules of *P. santalinus* show pharmacological activity, e. g., anti-inflammatory, anti-ulcer, anti-cancer as well as antioxidant activity. Future systemically designed studies might be very promising and could lead to the development of phytopharmaceutical drugs or herbal formulations (Dahat et al. 2021).

##### anti-inflammatory activity

Dahat et. al (2021) demonstrated in a study the anti-inflammatory potential of benzofurans and neoflavanoids, that were isolated from a dichloromethane fraction of heartwood

methanolic extract. The compounds showed either significant inhibition of inflammatory markers such as elastase or of superoxide anion release from neutrophils.

Another study by Sankaran et. al (2021) investigated the potential therapeutic activity against adipogenesis and adipogenesis- induced inflammation in a 3T3-L1 cell culture model with a chloroform bioactive fraction of *P. santalinus* (CFP). LPS-induced 3T3-L1 cells with dose-dependent treatment of CFP showed a significant reduction in TNF $\alpha$  and IL-6. In gene expression studies a down regulation of messenger (m)RNA expression of peroxisome proliferator-activated receptor- $\gamma$  (PPAR- $\gamma$ ), leptin, TNF- $\alpha$  and IL-6 and sterol regulatory element-binding protein-1c (SREBP-1c) could be observed. In conclusion, these results suggest that *P. santalinus* shows anti-inflammatory activity and further research in this field is crucial.

#### antioxidant activity

*P. santalinus* contains polyphenolic compounds, that are traditionally used in the treatment of diseases involving oxidative stress (Dahat et al., 2021). In vitro studies of the methanolic extract of the leaves displayed radical-scavenging activity for nitric oxide (NO), hydrogen peroxide and 1,1-diphenyl-2-picrylhydrazyl (DPPH). Other studies using methanolic extract of heartwood also showed DPPH radical-scavenging activity as well as Fe<sup>3+</sup>-reducing capacity. Reports also confirmed *in vitro* antioxidant activity against free radicals of pterostilbene. Further proving studies using the heartwood are needed (Bulle et al., 2016).

#### anti-cancer activity

Bioactive compounds isolated from *P.santalinus* show cytotoxic and anticancer activity. Cervical adenocarcinoma cells were treated with a methanolic extract of *P. santalinus* which resulted in growth inhibition and induction of apoptosis through the mitochondrial pathway via cytochrome-c release and activation of the caspase pathway as well as degradation of PARP (peroxisome-activated receptor protein). Other studies showed that benzofuran compounds display cytotoxicity against Ca9-22 cancer cells, and savinin showed a high inhibition potential on T cell proliferation (Bulle et al., 2016)

#### anti-ulcer activity

A study on Wistar male albino rats showed that an ethanolic extract of *P. santalinus* heartwood led to prevention of mitochondrial dysfunction by scavenging free radicals and

maintaining ATP levels and preventing severe depletion of arachidonic acid. It was also able to prevent nonsteroidal anti-inflammatory drugs (NSAID) induced damages in gastric mucosa as well as degranulation of mast cells (Dahat et al., 2021).

## **4.2 Inflammation and inflammatory diseases**

Inflammation is a vital response induced by infections, tissue injuries or challenging antigens in order to repair damaged tissue or eradicate microbes and irritants. However, excessive inflammation may cause severe problems such as tissue damage, organ dysfunction and even death (Sherwood & Toliver-Kinsky 2004). The inflammatory reaction acts as a key role in several maladies, such as cardiovascular, neurodegenerative, gastrointestinal diseases as well as joint and skin disorders. Inflammatory cytokines, including interleukin 1 (IL), tumor necrosis factor (TNF) and lipopolysaccharide (LPS) provoke the expression of proinflammatory genes, e.g., adhesion molecules and chemoattractants. This leads to the adherence and transmigration of immune cells through the endothelium into the underlying tissue and migration toward the site of injury. Induced genes are adhesion molecules (VCAM-1, ICAM-1), E-selectin, cytokines (IL-1, IL-8, IL-6), cyclooxygenase, anti-apoptotic proteins, chemokines and their receptors and A20 (an early NF $\kappa$ B response gene). The transcription factor NF $\kappa$ B plays a main role in this process. Many studies already confirmed that inhibiting NF $\kappa$ B, prevents or at least attenuates the proinflammatory gene expression (Lammel et al., 2020).

Although numerous steroidal and non-steroidal anti-inflammatory drugs are currently available, there are also certain limitations for their use, especially for chronic-diseases, suggesting that novel-lead structures are needed. Natural products have not only long been traditionally used for treatment of inflammatory diseases, but also offer a rich source for novel secondary metabolites, that interfere with key players in inflammation (Lammel et al., 2020; Zwirchmayr et al., 2020)

### **4.2.1 Acute Inflammation**

Acute inflammation is caused by the immune system as a response reaction to different kinds of noxae, including microbial (viral or bacterial) stimulation, but also physical, chemical, or mechanical stimuli. Examples for these latter stimuli are UV-irradiation, tissue necrosis, burning or frost bites, which are also designated as sterile inflammation. The five key signs of

inflammation are heat, redness, swelling, pain, and loss of function, caused by various vascular effects. Several vascular events occur during inflammation. Firstly, the relaxation of the smooth muscle cells causes vasodilation and an increase in blood flow into the capillaries. Secondly, vascular permeability increases, therefore more fluid can exude into the connective tissue, resulting in the formation of edema and swelling. Pain and itching arise due to the release of chemical agents and lastly, leucocytes emigrate into inflamed tissue. This is managed by the expression of adhesion molecules on endothelial cells (EC) and secretion of chemo attractants (de Martin, 2019).

The innate immune-system is mediated by macrophages, natural killer cells, CD8+T-lymphocytes and neutrophils and acts as an early response to harmful stimuli. It serves a crucial role in the activation of inflammation by releasing pro-inflammatory cytokines, chemokines, nitric oxide (NO) and tissue factors. Additionally, microbial antigen presentation (primary controlled by CD4+T-lymphocytes) activates the adaptive immune system and further amplifies the acute inflammation process (Sherwood & Toliver-Kinsky, 2004).

#### **4.2.2. Chronic inflammation**

There is no doubt that such a complex and powerful response, as the inflammatory, must be tightly controlled. Otherwise, a prolonged duration may develop, leading to chronic inflammation. In chronic inflammation, tissue destruction, acute inflammation as well as attempts at tissue repair occur simultaneously (Sherwood & Toliver-Kinsky, 2004). Up until now, unfortunately, it is barely understood how an acute inflammation turns into chronic state. Therefore, prospective research in this field might be crucial, as chronic inflammation is an indicator for several diseases. These include illnesses of the skin (psoriasis), the joints (rheumatoid arthritis), the intestine (ulcerative colitis), the lung (asthma), the blood vessels (arteriosclerosis), the central nervous system (Alzheimer, multiple sclerosis), as well as many others (de Martin, 2019).

#### **4.2.3 NF $\kappa$ B signaling pathway**

Nuclear factor (NF)  $\kappa$ B is a family of transcription factors that play a critical role in inflammatory gene expression in EC. Part of the family are RelA (p65), RelB, NF- $\kappa$ B1 (p50), NF- $\kappa$ B2 (p52) and c-Rel. P50 and p52 are synthesized from p105 and p100, inactive precursor molecules, as well as their inhibitory subunits I (inhibitor)  $\kappa$ B $\alpha$ , I $\kappa$ B $\beta$ , and I $\kappa$ B $\epsilon$ . These subunits



form homo- and heterodimers, with the most common one being p65/p50. NF $\kappa$ B was originally found in B cells but is now known to be present in various cell types, especially in cells of the immune system. It can be activated rapidly and transiently, which is essential for the expression of immune-response genes. These must be upregulated, only when needed, for a certain time and afterwards shut down immediately. Conversely, due to persistent stimulating agents or through defective mechanisms of downregulation, prolonged activation of NF $\kappa$ B is possible, which is the reason for many chronic inflammatory as well as vascular diseases (de Martin et al., 2000)

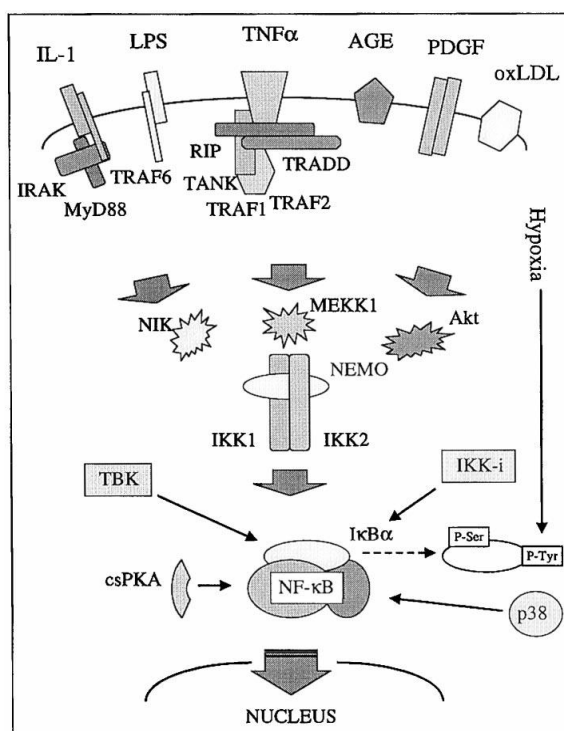


Figure 3 NF $\kappa$ B signaling pathway

Figure 3 illustrates the NF $\kappa$ B signaling pathway. In the cytoplasm, NF $\kappa$ B dimers persist in an inactive form, due to interaction with I $\kappa$ B. It can be activated very rapidly through inflammatory and other stimuli that lead to phosphorylation, ubiquitination, and degradation of I $\kappa$ B $\alpha$ . Notable stimuli are TNF, LPS, interleukin (IL)-1 as well as advanced glycation end products (AGEs), platelet-derived growth factor (PDGF) and oxidized lipids. By binding to their receptors on the cell surface cytoplasmatic receptor-specific adapter molecules (e.g., TRAF1/2) assemble. These can activate various kinases like MAP3 kinases (TAK1, NIK, MEKK1) which further activate IKKs that phosphorylate I $\kappa$ B causing its degradation. Hence, NF $\kappa$ B is now able to translocate into the nucleus and to mediate the expression of proinflammatory and other genes (de Martin et al., 2000).

#### 4.2.4 HSPA1A and its role in oxi-inflamm-aging

The expression of HSPA1A, a member of the heat shock protein 70 family, is induced under stress conditions, which acts as a cellular defense mechanism (de Toda et al., 2016). Decreased induction has been related to aging, while increased expression was connected to longevity. The oxidation-inflammation theory of aging states, that the core age-related alterations of body cells are chronic oxidative stress and inflammatory stress situations, causing higher levels of oxidant and inflammatory compounds and lower anti-inflammatory and antioxidant defense mechanisms. Hence, Hsp70 might be an important regulator of the rate of aging, based on inflammation and oxidation being interlinked processes and Hsp70 showing protection against harmful effects of oxidative stress and modulating the inflammatory status. The role might differ in mitotic and post-mitotic tissues, as they also show differences in their age-related mechanisms of response (de Toda & de la Fuente, 2015). De Toda et al. (2016) were able to show that in long-lived mice the HSPA1A levels are similar to those from adult mice, while prematurely aging mice showed HSPA1A levels similar to those in chronologically old mice. This demonstrates, that HSPA1A levels are preserved in long-lived animals and shows the possibility of age-associated and tissue specific variations. Zhao et al. (2005) investigated the correlation of heat shock protein expression and lifespan extension on *Drosophila*. Their results showed a positive correlation between higher Hsp70 and Hsp 22 RNA-levels and long-lived flies, also suggesting a close correlation between Hsp-expression and longevity in *Drosophila melanogaster*.

### 4.3. Cell culture as an *in vitro* study model

#### 4.3.1 HUVEC primary cells

HUVEC (human umbilical vein endothelial cells) are endothelial cells, that are isolated from human umbilical veins (Su et al., 2020). HUVECs are primary cells and thus more similar to the *in vivo* state and normal physiology, as they derive directly from tissue and are not immortalized. For this reason, HUVECs provide a well suitable model system for studying the effects of drugs and toxic compounds on endothelial cells (Egger et al., 2013).

With HUVEC, studies of the physiological and pathological effect of various stimuli, either isolated or in coculture are possible, as it physiologically represents the human vascular

endothelium. The human endothelium builds an important barrier between blood and tissue and is responsible for the transfer of hormones, nutrients, white blood cells and anti-inflammatory responses. Therefore, HUVEC models are used for studies of biological processes and diseases such as inflammation, apoptosis, cancer and cardiovascular diseases. Moreover, in HUVECs that are in the state of confluence, cell proliferation is greatly inhibited, meaning that they are subject to contact inhibition and limitations in growth density. While working with these cells, gender differences must be considered, as human umbilical veins are fetal and not maternal. Some other disadvantages that need to be considered are that EC growth is much higher *in vitro* than *in vivo*. This can be controlled by using inhibitors and growth factors. Finally, HUVECs cannot be used for long-term experiments since they have a limited lifespan of around 10 passages and might even lose their primary characteristics and ability to respond to stimuli after passage 6 (Medina-Leyte et al., 2020).

#### Morphological description of HUVEC

HUVECs form a monolayer of polygonal cells. Characteristics for EC are pinocytic vesicles, small fibrils near the ellipsoid nucleus, tubular shaped mitochondria and 1 to 3 nucleoli present in the nucleus. While growing cell-cell contact occurs and a basement membrane layer is formed, a hexagonal or cuboidal confluent monolayer form is present with slightly overlaying nuclei. Cells in confluence show elongated rather than cuboidal cells as the monolayer decreases (Medina-Leyte et al., 2020).

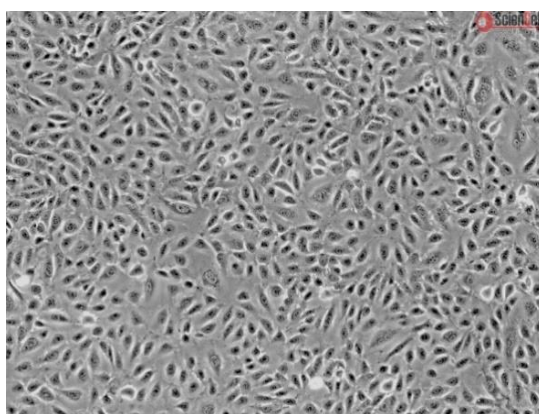


Figure 4 Human Umbilical Vein Endothelial Cells

#### 4.3.2. HEK-293 cells

The HEK (human embryonic kidney) cell line is a permanently transformed cell line, that originally descended from the kidney of an aborted human embryo from 1973. It was modified by transformation with sheared Adenovirus 5 DNA, that integrated into chromosome 19. This led to the expression of E1A/E1B proteins, which inhibit apoptosis by interfering with the cell cycle control pathways. HEK-293 cells are widely used in various experiments such as protein interaction studies, signal transduction and protein expression or biopharmaceutical production studies (Thomas & Smart, 2005; Lin et al., 2014) Yin et al. (2014) proved through a comprehensive genomic characterization of the 293 cell-line that as long as the cells are handled according to standard cell cultivation procedure, they are still stable after multiple passaging and also after distribution and cultivation in various laboratories.

##### Morphological description of HEK-293 cells

HEK-293 cells have a round, lightly granular shape. At confluence they often appear polygonal, which suggests an epithelial character (Valerius et al., 2002). At 50%-70% confluence HEK-293 cells remain biochemically active, when reaching 70 % confluence, cells can be seeded at 30-50% density for further experiments including transfections. Cells, which have been growing for a period of 36-48 hours through multiple cell divisions, form micro-islands with individual cells, that are coupled to each other through gap junctions (Thomas & Smart, 2005).

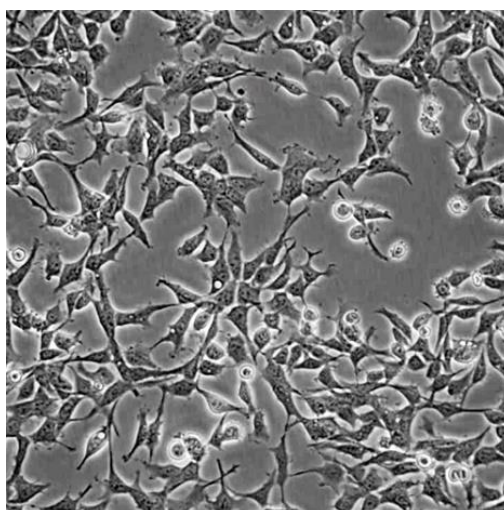


Figure 5 HEK-293 cell line

## 5. Results and Discussion

### 5.1 Pharmacological investigation of *Pterocarpus santalinus* in HUVEC cells

The aim of this diploma thesis is to investigate the potential anti-inflammatory and anti-ageing effect of *P. santalinus*. Previous studies of plant-based drugs that are traditionally used for the treatment of inflammation, show anti-inflammatory activity through NF $\kappa$ B inhibition as for example demonstrated by Zwirchmayr et al. (2020) for masterwort. Therefore, extracts from *P. santalinus* were analyzed for their anti-inflammatory activity and potential NF $\kappa$ B inhibition. This was conducted through stimulation of HUVEC with various stimuli and examination of downregulated or upregulated genes, that play a critical role in the inflammatory process. Endothelial cells were chosen as the *in vitro* study model due to their importance during inflammatory reactions. Through the secretion of proinflammatory cytokines and through their role in leukocytes migration they act as a key factor in the inflammatory process (Lammel et al., 2020). HUVECs were directly isolated from umbilical cords and used up until passage 5. By being primary cells the advantage of mimicking the *in vivo* state and physiology were given (Egger et al., 2013).

The sandalwood extract was prepared at the Department of Pharmacognosy at University of Vienna. A large-scale extract of *P. santalinus* heartwood (PtesanXDM) was obtained. The dried extract (PS) was dissolved in dimethyl sulfoxide (DMSO) and stored at -20 °C (Zwirchmayr et al., 2020). Thrakl (2019) provides a detailed description of the extraction in her diploma thesis.

#### 5.1.1 Dose response study with TNF and LPS

Previous studies by Natalia P. and Rudžionytė I. have demonstrated an inhibitory effect of PS in IL-1 stimulated HUVEC, involving inhibition of NF $\kappa$ B (submitted Natalia et al., 2021). In order to extend these studies to other inflammatory stimuli, the effect of PS on TNF and LPS stimulation was investigated. First, efficient concentrations of the inflammatory agents for stimulation of the endothelial cells were determined using dose response studies of TNF and LPS.

The experiment was conducted in triplets and cells were used up until passage 5. Cells were plated in 12 well plates and after growing to post confluency, stimulated with either 1 ng/ml LPS, 10 ng/ml LPS, 100 ng/ml LPS or 1000 ng/ml LPS. As a control, cells were kept unstimulated. After stimulation, cells were incubated for 2 hours, before their mRNA was extracted, using the Peq Gold total RNA isolation Kit by VWR. 1 µg of mRNA was then reverse transcribed into cDNA by using random hexamers and murine leukemia virus reverse transcriptase. With the cDNA real-time PCR (polymerase chain reaction) was performed with a SYBR green supermix. TRAF1 and CX3CL1 were chosen as read-out since these were the top PS-regulated genes in response to IL-1. The relative mRNA expression was normalized to GAPDH. To calculate the fold change  $2^{-\Delta\Delta Ct}$  method (Livak & Schmittgen, 2001) was used and the results show mean fold induction of averaged Ct values.

The same procedure was conducted for TNF with 0,05 ng/ml, 0,5 ng/ml, and 5 ng/ml.

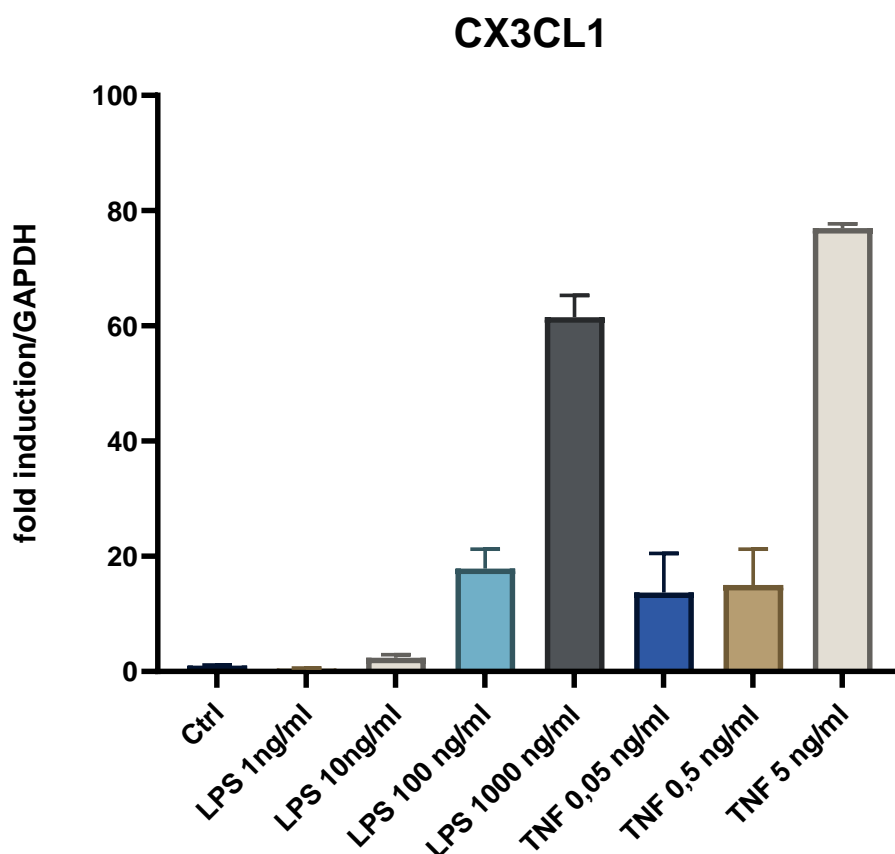


Figure 6 Real time PCR analysis for CX3CL1 with different concentrations of LPS. and TNF

CX3CL1 also known as fractalkine is a chemokine, a chemoattractant protein, that is responsible for the recruitment of inflammatory cells at the site of inflammation. In contrast to other chemokines, CX3CL1 has unique structural and functional characteristics and is known to play an important role in inflammation (Jones et al., 2010). Figure 6 shows the up-regulation of CX3CL-1 in endothelial cells through stimulation with various concentrations of LPS/TNF. LPS at 1 ng/ml shows no induction, while LPS 1000 ng/ml shows a relatively high fold induction of around 61 (figure 6). Thus, for further experiments 500 ng/ml LPS was used for stimulation.

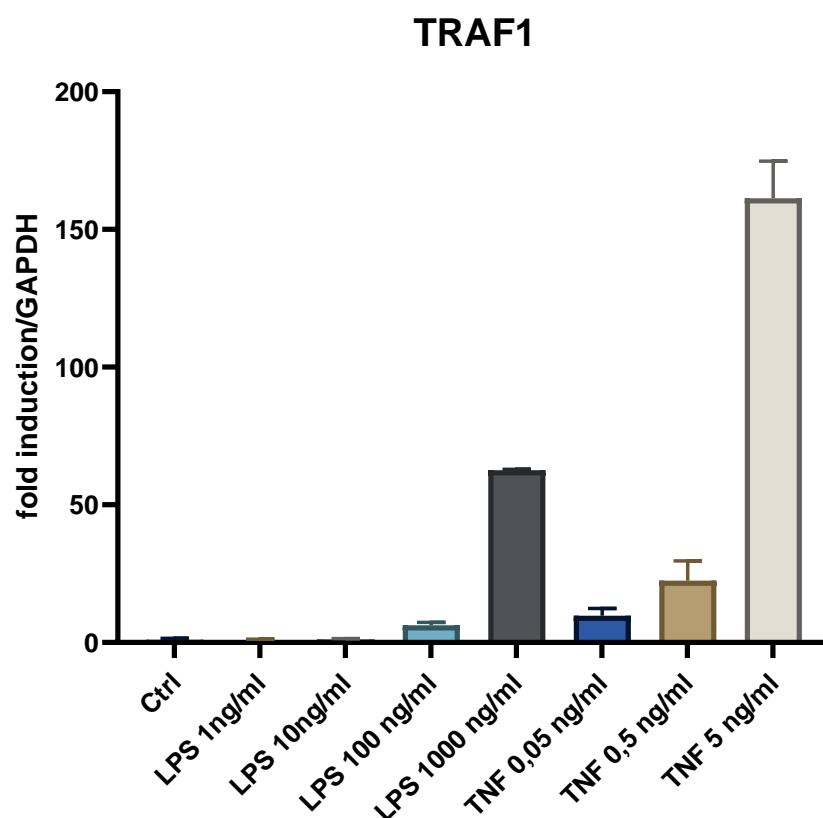


Figure 7 Real time PCR analysis for TRAF1 with different concentrations of LPS and TNF

TRAF1 (Tumor necrosis factor receptor-associated factor 1) is an NF- $\kappa$ B inducible protein that bridges the cytoplasmic part of the TNF receptor to IKK2 (Sughra et al., 2019). It also plays an important role as a feedback loop for TNF but also LPS signaling (Abdul-Sater et al., 2018). It has a diverse role in human health as it plays a key role in the immune system as a signaling

molecule but is also overexpressed in several diseases, like B cell related cancers (Edilova et al., 2018).

Figure 7 displays the upregulation of TRAF 1 through stimulation. Both charts show similar progressions, only for TRAF1 the fold induction was generally higher compared to CX3CL1.

### 5.1.2 Kinetic analysis

Kinetic analyses were performed for LPS and TNF to examine the stimulation over a certain period of time. The experiment was again conducted in triplets and cells were used up until passage 5. Cells were plated in 12 well plates and grown until post confluency. For the experiment they were either pretreated with 50 µg/ml PS for 30 minutes and subsequently stimulated with 500 ng/ml LPS or with 2,5 ng/ml TNF and incubated for either 0, 0,5, 1, 3, or 6 hours. For positive control, cells were stimulated without pretreatment with PS and as negative control, cells were kept untreated and unstimulated. In the experiment with TNF, another control of cells, that were treated with 50 µg/ml PS but without subsequent stimulation, was also implemented. Afterwards, the mRNA was extracted, by using the Peq Gold total RNA isolation kit by VWR. 1 µg mRNA was reverse transcribed into cDNA using random hexamers and murine leukemia virus reverse transcriptase. With the cDNA real time PCR was performed with a SYBR green supermix and with various primers, that are involved in the inflammatory process. The relative mRNA expression was normalized to GAPDH. To calculate the fold change  $2^{-\Delta\Delta C_t}$  method (Livak & Schmittgen, 2001) was used and the results show mean fold induction of averaged  $C_t$  values.

The following genes were chosen based on an expression profiling experiment conducted previously (submitted Natalia et al., 2021).

#### Downregulated genes in TNF stimulated endothelial cells

The following figures show examples of downregulated genes in 2,5 ng/ml TNF stimulated endothelial cells through treatment with 50 µg/ml PS.



### CX3CL1

Figure 8 displays the results for CX3CL1. TNF stimulated cells showed the highest expression of CX3CL1 around 3 hours after stimulation. PS treatment strongly inhibited gene expression. CX3CL1 levels could be reduced by 96 %.

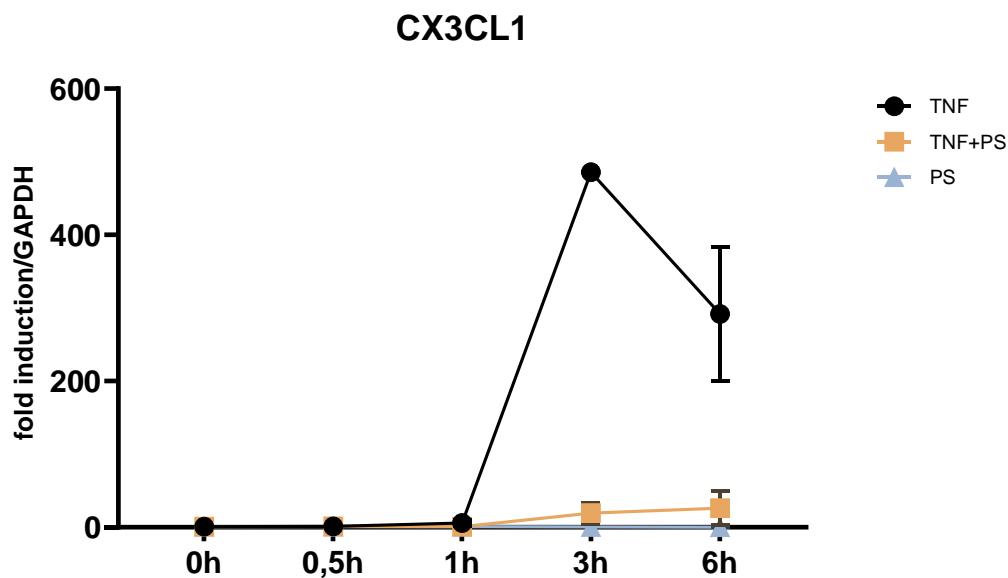


Figure 8 Real time PCR analysis for CX3CL1 with 2,5 ng/ml TNF and with or without treatment with 50 µg/mL PS

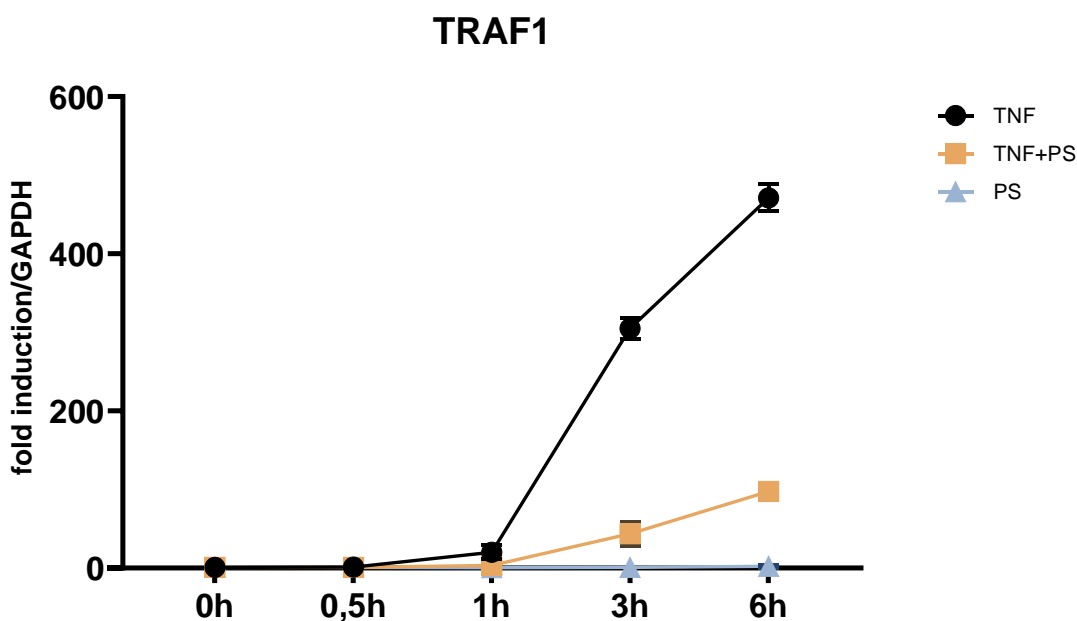


Figure 9 Real time PCR analysis for TRAF 1 with 2,5 ng/ml TNF and with or without treatment with 50 µg/mL PS

## TRAF1

Figure 9 shows the progression for TRAF1 in stimulated endothelial cells. Through treatment with PS, fold induction was massively reduced, displaying the decreased expression of TRAF1. TRAF 1 levels could be massively reduced by 99 %.

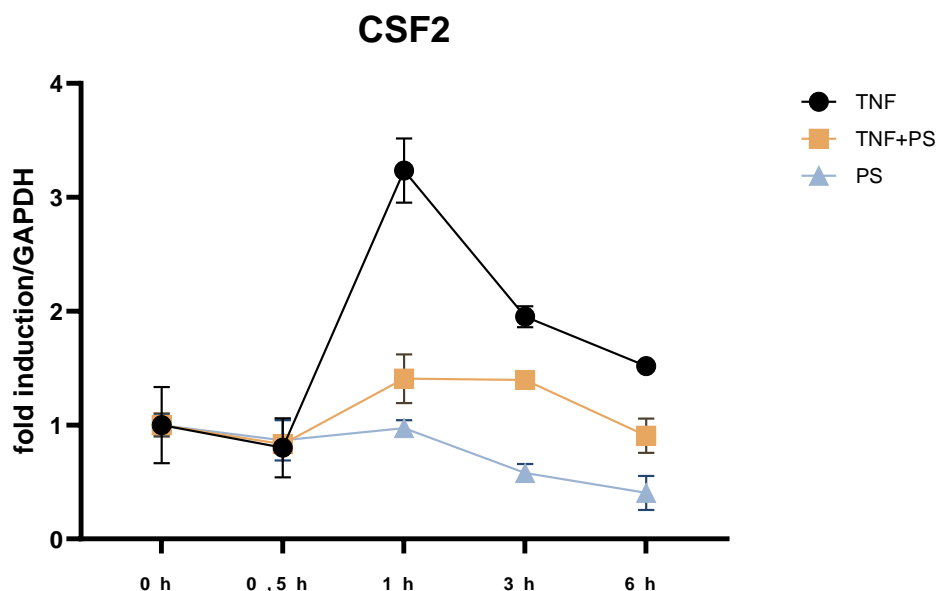


Figure 10 Real time PCR analysis for CSF2 with 2,5 ng/ml TNF and with or without treatment with 50 µg/mL PS

## CSF 2

GM-CSF (granulocyte macrophage colony-stimulating factor) also known as CSF2 is a cytokine responsible for macrophages activation and for their differentiation towards a proinflammatory phenotype. Various cells, like fibroblasts, macrophages, endothelial cells produce GM-CSF during inflammatory/autoimmune processes. CSF2 expression is induced through proinflammatory cytokines, including TNF or IL-1. It plays a key role in proinflammatory processes by recruiting myeloid cells and enhancing their activation and survival (Ushach & Zlotnik, 2016).

In figure 10 the upregulation of CSF2 through TNF stimulation is shown, it was highest 1 hour after stimulation and afterwards decreases. PS treatment strongly diminished CSF2 expression. The fold induction of cells pretreated with PS was way lower at around 1,5 compared to fold induction of cells stimulated with TNF without prior PS treatment.

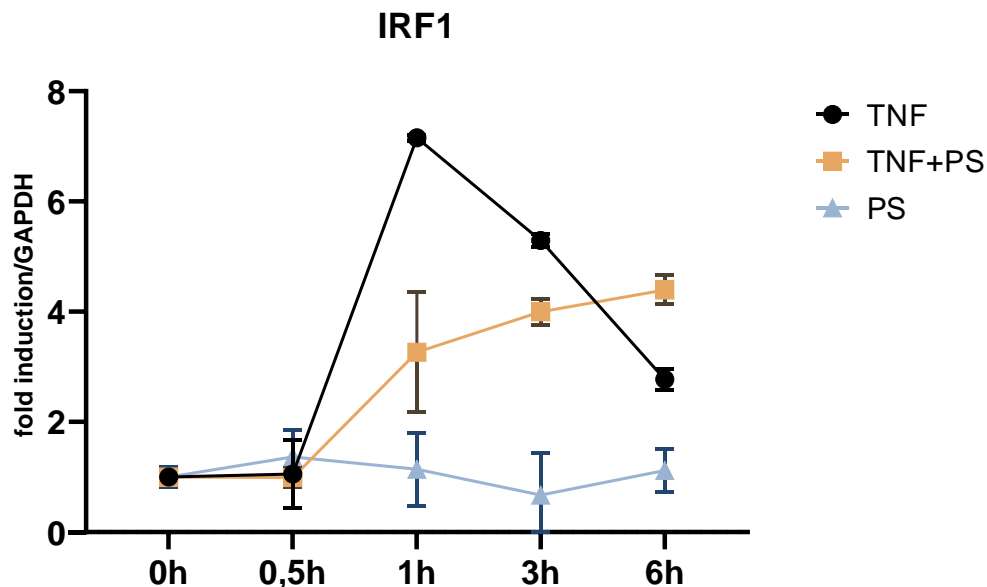


Figure 11 Real time PCR analysis for IRF1 with 2,5 ng/ml TNF and with or without treatment with 50  $\mu$ g/mL PS

#### IRF1

Interferon regulatory factor 1 (IRF1) is a nuclear factor, binding and activating promoters of interferon genes of type 1. It plays a crucial role in pathogenesis and in immune response processes. The IRF 1 gene is regulated by various stimuli, including interferons and NF $\kappa$ B (Feng et al., 2021). IRF1 cooperates with NF $\kappa$ B and induces the transcription of VCAM-1 in the inflammatory process (Neish et al., 1995).

Figure 11 displays the overexpression of IRF1 through TNF stimulation which reached its maximum one hour after stimulation. Due to PS treatment, the IRF 1 expression in the first hours after stimulation was diminished. Afterwards the inhibition seemed to become weaker.

#### VCAM1

Vascular cell adhesion molecule-1 (VCAM-1) is a cell adhesion molecule, that is vital for transendothelial migration of leucocytes by regulating inflammation-associated vascular adhesion (Kong et al., 2018) Its expression is induced by proinflammatory cytokines including TNF (figure 12). In endothelial cells pretreated with PS before stimulation, the expression of VCAM-1 was strongly diminished. Gene levels were reduced by 99 %. VCAM1, CX3CL1 and TRAF1 were the genes mostly effected by PS.

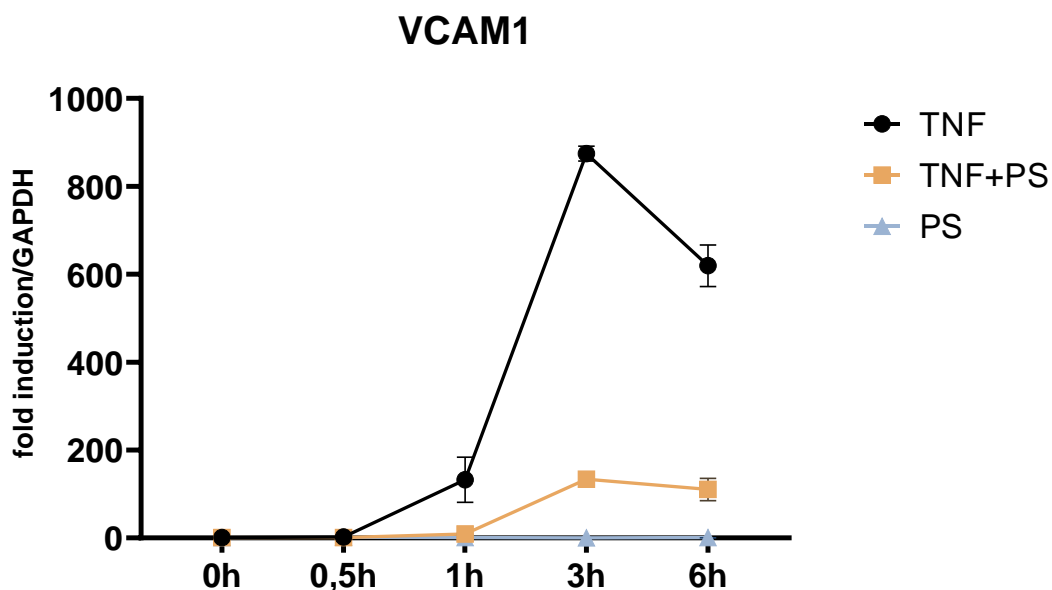


Figure 12 Real time PCR analysis for VCAM1 with 2,5 ng/ml TNF and with or without treatment with 50  $\mu$ g/mL PS

In inflammatory processes, VCAM-1 and other adhesion molecules are responsible for recruiting leukocytes at inflamed sites through leukocyte adhesion. Recent studies also suggest that VCAM-1 is associated with several immunological disorders like rheumatoid arthritis. Under chronic condition of some maladies, VCAM-1 is not only expressed in endothelial cells, but also on the surface of other cells including dendritic cells or myoblasts (Kong et al., 2018)

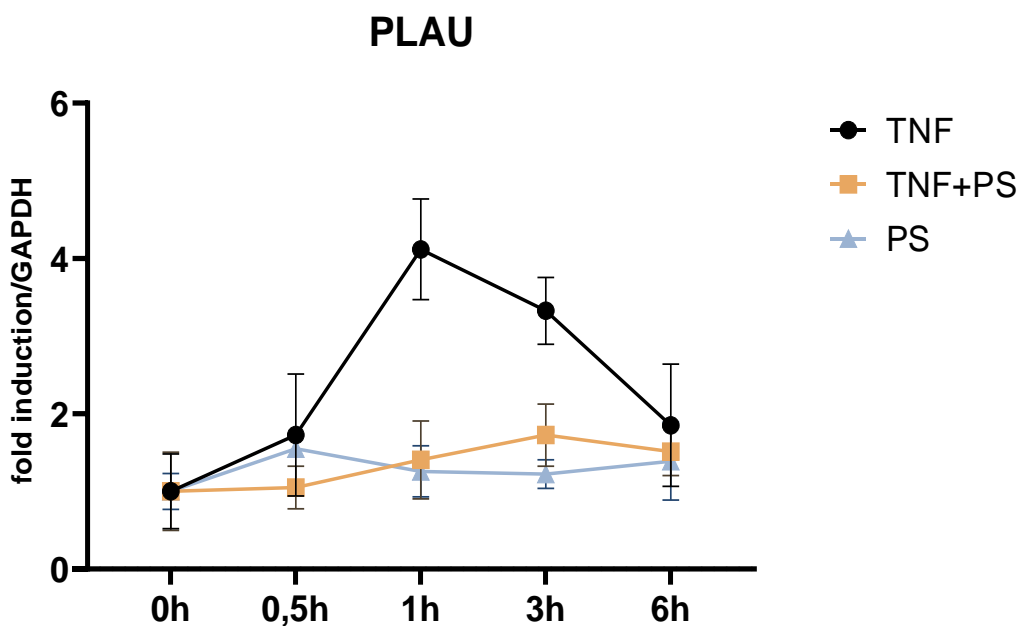


Figure 13 Real time PCR analysis for VCAM1 with 2,5 ng/ml TNF and with or without

#### PLAU

Plasminogen activator urokinase (PLAU) is involved in the conversion of plasminogen to plasmin and also in several biological processes including angiogenesis, promotion of vascular permeability and proteolysis of extracellular matrix-remodeling proteins (Park et al., 2021).

Figure 13 shows that PLAU is also a TNF responsive gene and through treatment with PS the gene expression was strongly reduced.

### Downregulated genes in LPS stimulated endothelial cells

The following figures are examples of downregulated genes in 500 ng/ml stimulated endothelial cells through treatment with 50  $\mu$ g/ml PS.

Besides TNF, bacterial lipopolysaccharide also activates the expression of a similar set of genes in endothelial cells. TNF and LPS signaling pathways differ in the initial stages, but converge at the IKK complex, leading to NF $\kappa$ B (Mercurio et al.,1997). Considering, that *P. santalinus* acts at least partially through NF $\kappa$ B inhibition, it was investigated whether PS also inhibits LPS stimulated gene expression. The response in LPS stimulated cells, as shown in Figure, 14, 15 and 16, is slower compared to TNF stimulation. Through inhibition PS diminishes the expression of VCAM-1, TRAF 1 and CX3CL1. In comparison to TNF, it is less distinct over the 6 hours observed.

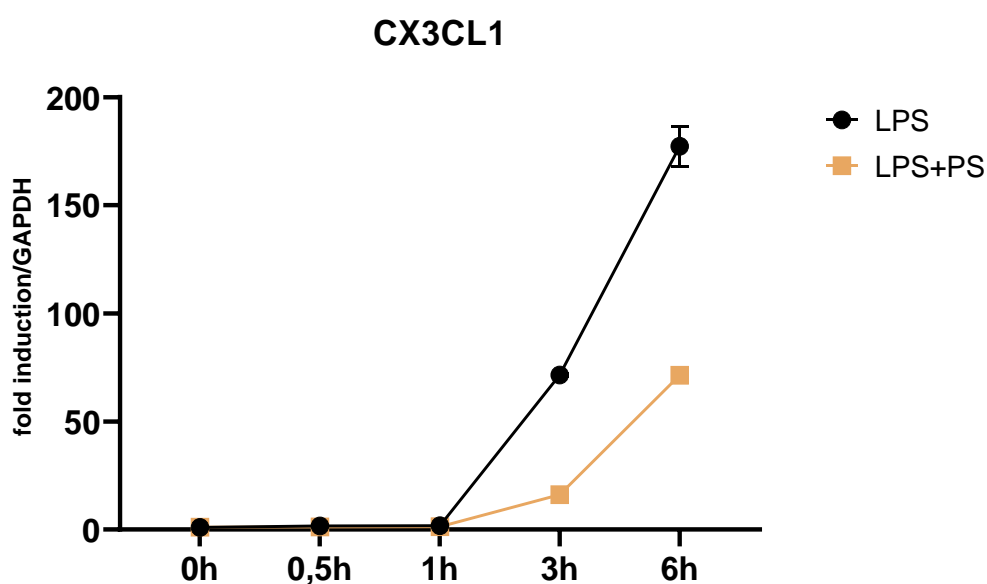


Figure 14 Real time PCR analysis for CX3CL1 with 500 ng/ml LPS and with treatment with 50  $\mu$ g/mL PS

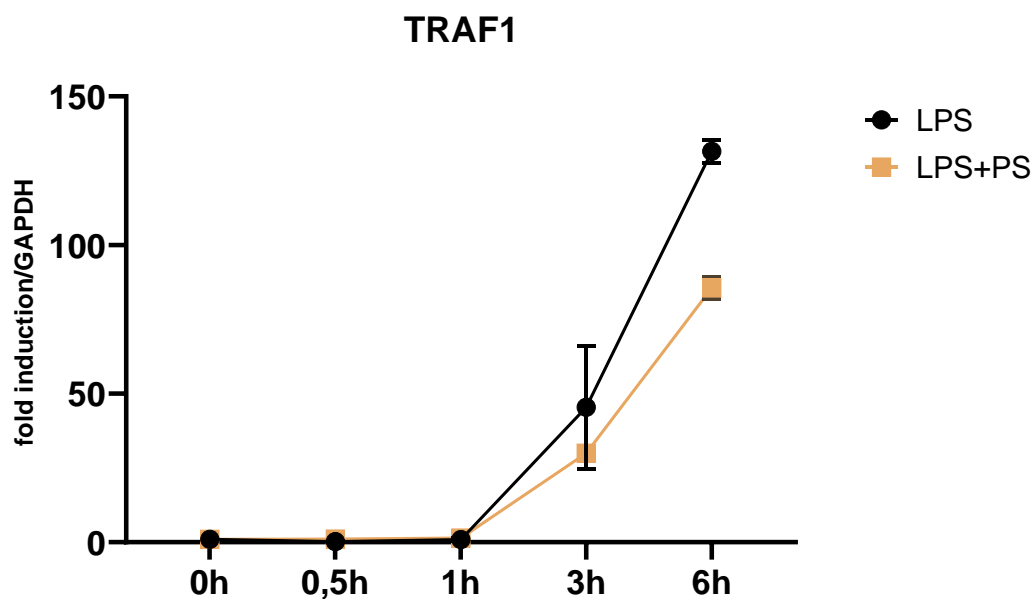


Figure 15 Real time PCR analysis for TRAF1 with 500ng/ml and with treatment with 50  $\mu$ g/mL PS

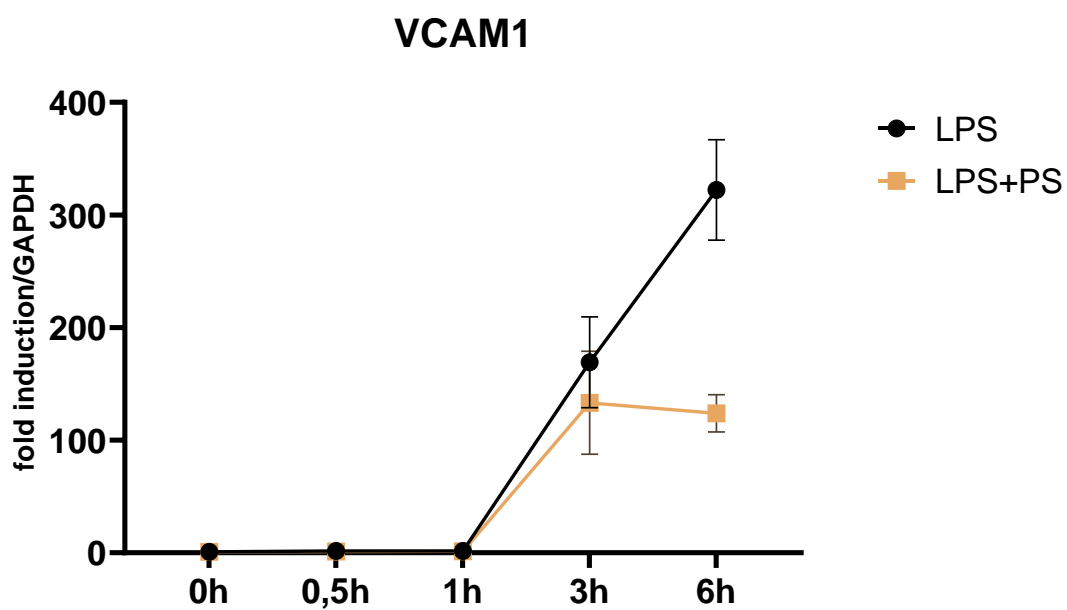


Figure 16 Real time PCR analysis for VCAM1 with 500ng/ml LPS and with treatment with 50  $\mu$ g/mL PS

### Upregulated genes in TNF stimulated endothelial cells

PS not only suppresses the expression of various genes involved in the inflammatory process, but it also enhances the expression of some. The figures below display examples of upregulated genes through PS treatment in 2,5 ng/ml TNF stimulated endothelial cells.

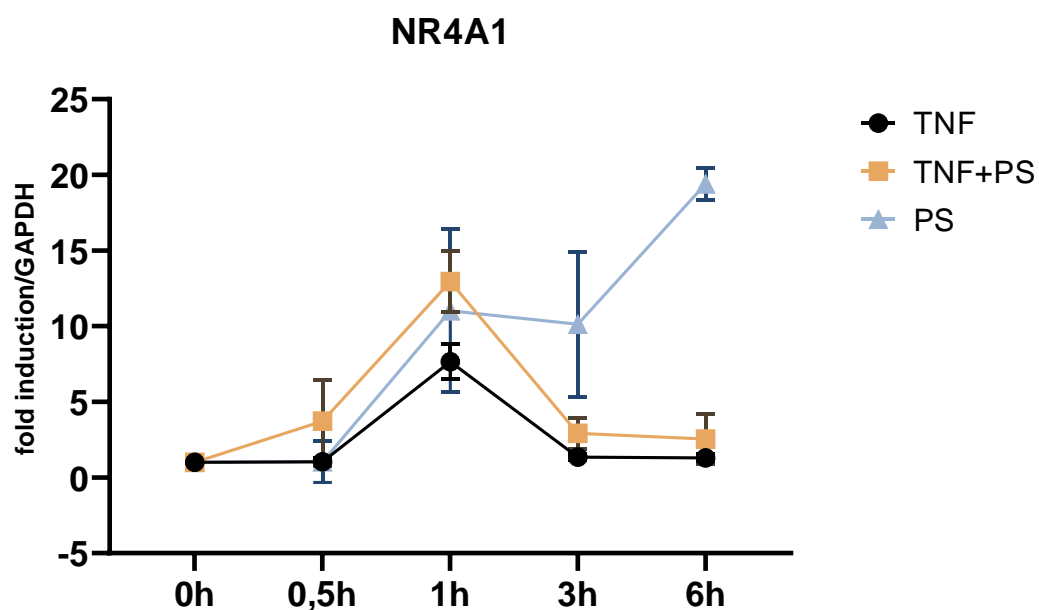


Figure 17 Real time PCR analysis for NR4A1 with 2,5 ng/ml TNF and with or without treatment with 50  $\mu$ g/mL PS

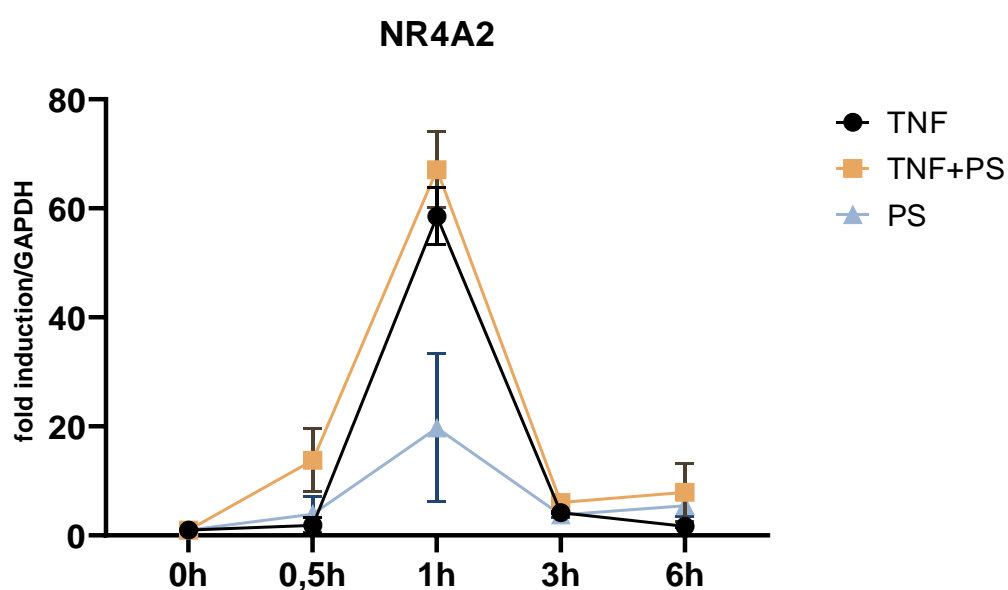


Figure 18 Real time PCR analysis for NR4A2 with 2,5 ng/ml TNF and with or without treatment with 50  $\mu$ g/mL PS



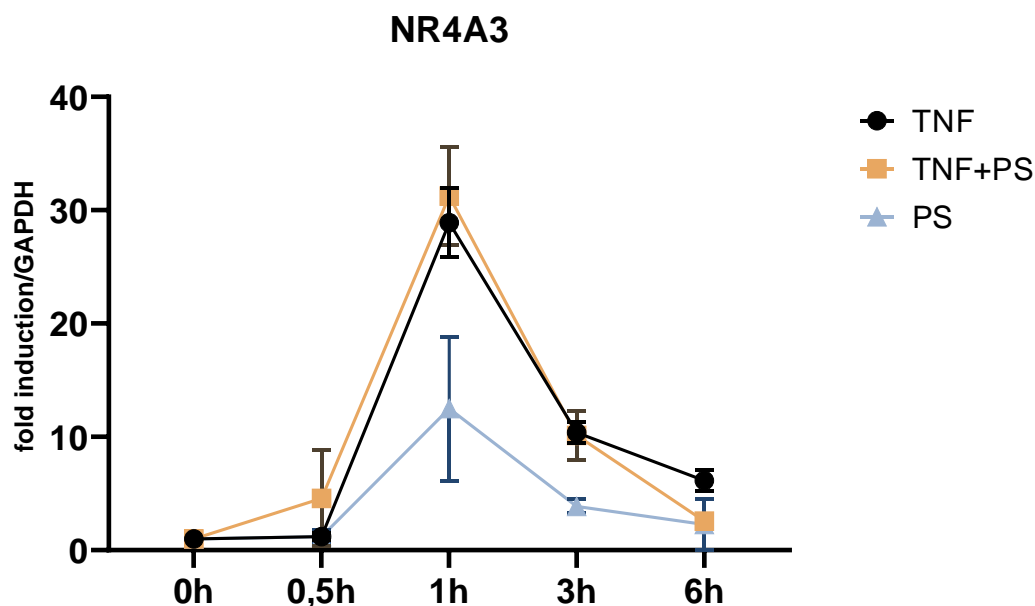


Figure 19 Real time PCR analysis for NR4A3 with 2,5 ng/ml TNF and with or without treatment with 50  $\mu$ g/mL PS

#### NR4A1, NR4A2, NR4A3

The nuclear receptors (NR) are a set of transcription factors, that are part of the steroid receptor superfamily and are essential in controlling cellular metabolism, proliferation and division in tissues (Lanig et al., 2015). The NR4A subfamily includes three members: NR4A1 (or nerve growth factor-induced gene B NGFI-B), NR4A2 (or nuclear receptor related protein 1 Nurr1) and NR4A3 (neuron-derived orphan receptor 1 NOR-1) (Martínez-González et al., 2021). Inducible NR4A expression is often regulated by NF $\kappa$ B (Han & Cao, 2012). NR4A1 is expressed and plays a crucial role in many physiological systems like the central nervous system, immune, endocrine, reproductive, respiratory, gastrointestinal and cardiovascular system (Lanig et., 2015). NR4A2 was known to be crucial for the maintenance of dopaminergic neurons. Recently, its critical role in some inflammatory diseases, by mediating multiple inflammatory signals, was discovered. (Han & Cao, 2012). NR4A3 is also known to play a relevant role in the function of inflammatory cells and in the immune response system (Martínez-González et al., 2021).

Figures 15 and 16 show similar progressions, the fold induction for NR4A2 was higher compared to NR4A3 and in both the maximum levels were reached after about one hour.

Treatment of HUVEC with PS alone showed induction of NR4A1, NR4A2 and NR4A3 expression. In stimulated endothelial cells, pretreatment with PS led to enhancement of NR4A expression.

### ZFP36, BHLH

ZFP36 belongs to a group of RNA binding proteins that regulate gene expression posttranscriptionally. ZFP36 exhibit anti-inflammatory activity by destabilizing mRNAs of cytokines (Galloway et al., 2016) as well as inhibiting NF $\kappa$ B (Schichl et al., 2009). Cook et al. (2020) describe the basic helix loop helix transcription factor (BHLH) E40 as an essential regulator of immunity during infections, inflammatory conditions, and autoimmunity, by regulating mouse and human CD4<sup>+</sup> T cells.

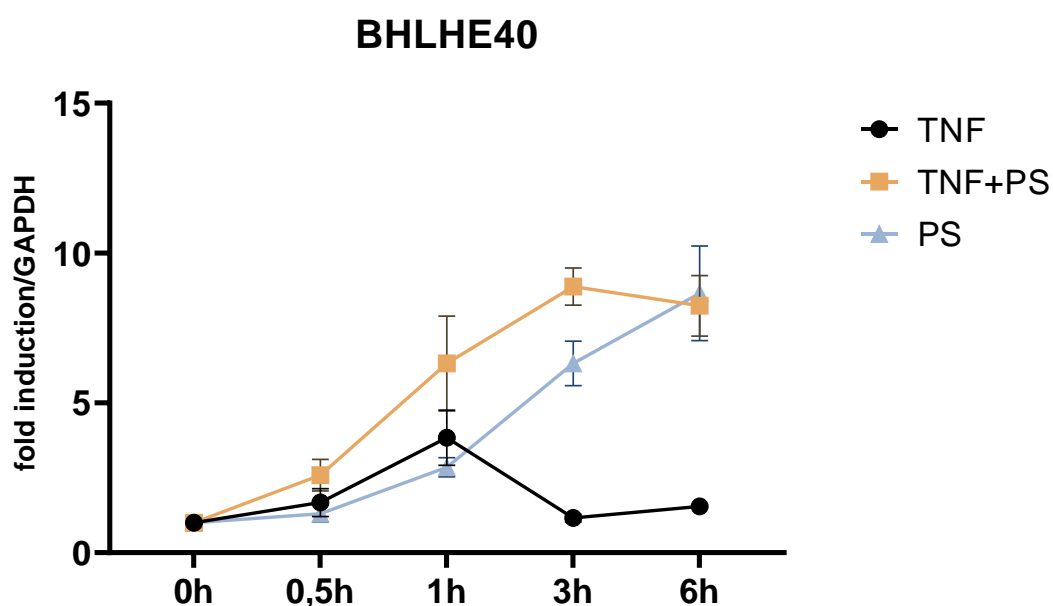


Figure 20 Real time PCR analysis for BHLHE40 with 2,5 ng/ml TNF and with or without treatment with 50  $\mu$ g/mL PS

ZFP36 (figure 21) expression was induced through PS treatment in endothelial cells. Stimulated HUVEC, that were pretreated with PS also showed higher expression of ZFP36 compared to HUVECs without PS treatment. One hour after treatment the expression was at its highest and diminished afterwards. Figure 20 displayed the real time PCR analysis for BHLHE40. PS again enhanced gene expression, for BHLHE40 over the entire observed period.

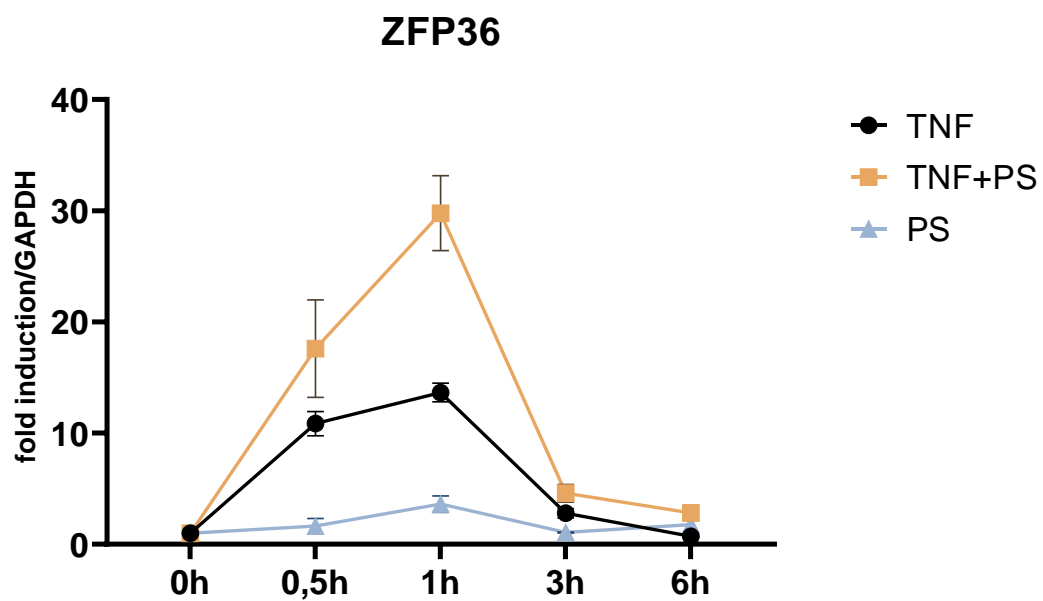


Figure 21 Real time PCR analysis for ZFP36 with 2,5 ng/ml TNF and with or without treatment with 50  $\mu$ g/mL PS

## 5.2. Pharmacological investigation of *Pterocarpus santalinus* in HEK-293 cells

Diploma student, Rudžionytė I. discovered in one of her experiments with *P. santalinus* upregulation of HSPA1A in HUVEC. For the following experiments upregulation of HSPA1A was tested in HEK-293 cells. The aim of this part of my thesis was to evaluate an alternative assay system. HEK-293 cells are permanently transformed and thus simpler to handle than primary cells. They can also be used after multiple passaging. For these reasons they provide a more simple experimental system that would allow the analysis of a large number of samples such as microfractions.

The potential anti-ageing effect of *P. santalinus* was examined by Thrakl (2019) in her diploma thesis, where she tested the lifespan extending potential in a *C. elegans* lifespan assay. The assay showed promising lifespan increasing results. A reason for the prolonged lifespan might be enhanced HSPA1A expression, as studies have linked increased expression with longevity (de Toda & de la Fuente, 2015).

### 5.2.1 Cell viability assay for PS in HEK-293 cells

First, the “CellTiter-Blue Cell Viability Assay” by Promega was performed to investigate the toxicity of PS on HEK-293 cells. The experiment was conducted in triplets and cells were plated in 96 well plates. Growing time was 2 days, afterwards cells were treated with different concentrations of PS (200/100/50/25/12,5/6,25/3,125 µg/ml). 4 µl of a lysis buffer was used as toxicity control. After treatment cells were incubated at 37 °C for 6 hours. Cell titer blue reagent was added to each well and cells were incubated for 2 more hours. To stop the reaction 3 % SDS (sodium dodecyl sulfate) was added. For the evaluation, fluorescence was read at 520/590 nm. The viability assay uses resazurin as an indicator, viable cells dispose the possibility to reduce resazurin into resorufin, which is highly fluorescent and can be measured (Promega, 2021).

Figure 21 displays, that none of the 6 concentrations used showed toxicity in HEK-293 cells. The control was probably relatively high, as all concentrations showed the same cell viability of around 80%.

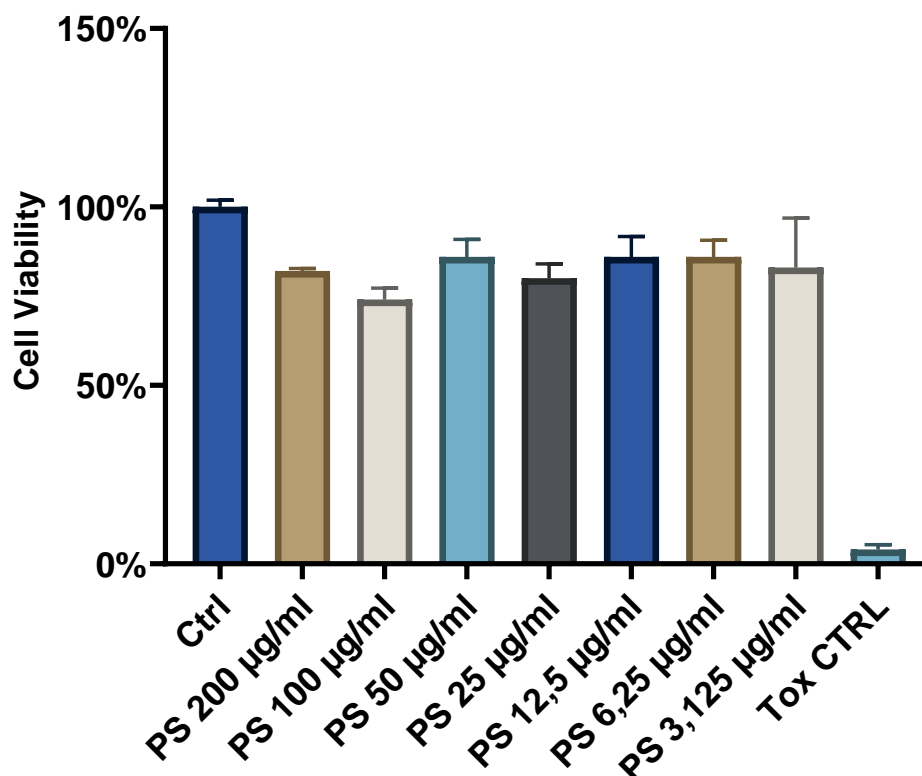


Figure 22 Cell Viability for different concentrations of PS in HEK-293 cells

### 5.2.2 Dose response study of PS in HEK 293 cells

In order to determine which concentration of PS enhances HSPA1A expression, a dose response study was conducted. The experiment was conducted in triplets, cells were plated in 12 well plates and after growing for 2 days treated with 50/25/12,5 and 6,25 µg/ml. Incubation time was 2,5 hours, afterwards mRNA was extracted by using the Peq Gold total RNA isolation kit by VWR. 1 µg mRNA was again reverse transcribed into cDNA using random hexamers and murine leukemia virus reverse transcriptase. With the cDNA real time PCR was performed with a SYBR green supermix with HSPA1A as a primer. The relative mRNA expression was normalized to GAPDH. To calculate the fold changed  $2^{-\Delta\Delta C_t}$  method (Livak & Schmittgen, 2001) was used and the results show mean fold induction of averaged Ct values.

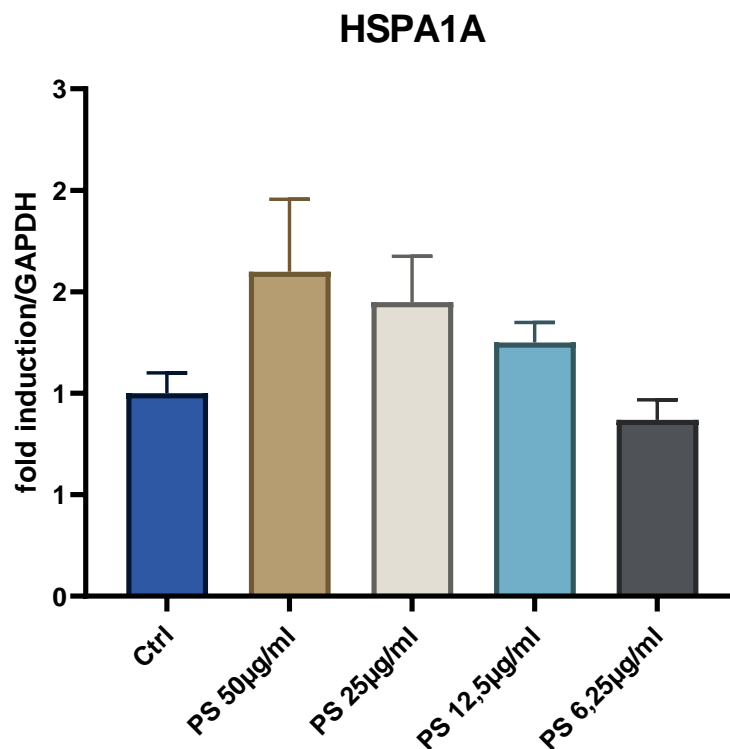


Figure 23 Real time PCR analysis for HSPA1A with different concentrations of PS

A dose dependent induction of HSPA1A expression was determined, visible by the changes in fold induction. For further experiment 50 µg/ml PS was used. In order to exclude amplification of the intronless heat shock sequences from potentially contaminating DNA, another real time PCR analysis was performed by using prior DNase treatment. Therefore, the Qiagen RNeasy Micro Kit was used for extracting mRNA. The results are displayed in Figure 24. The results showed again an amplification in HSPA1A expression; thus, DNA contamination could be excluded.

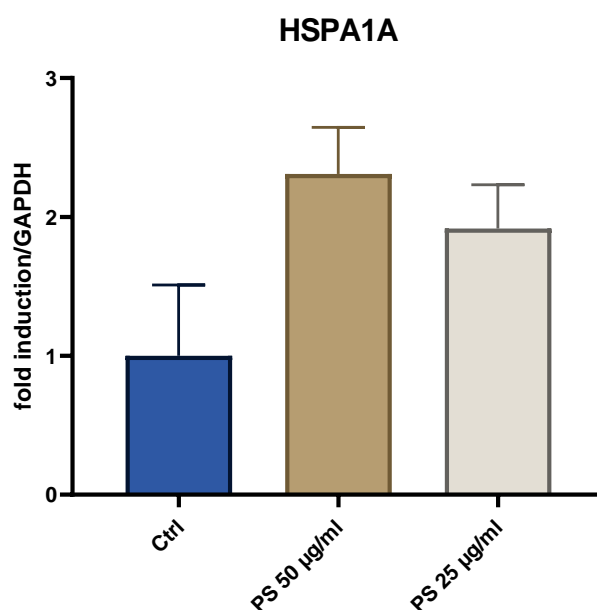


Figure 24 Real time PCR analysis for HSPA1A with 50/25 µg/ml PS in HEK-293 cells

### 5.2.3 Kinetic analysis of HSPA1A expression in HEK-293 cells

Kinetic analysis of HSPA1A expression were conducted to examine the expression over a certain period of time. The experiment was executed in triplets. Cells were plated in 12 well plates. After a growing time of two days, they were treated with 50 µg/ml PS and incubated for either 0,5/1/3 or 6 hours. The mRNA was extracted by using the Qiagen RNeasy Mini Kit. 1 µg mRNA was again reverse transcribed into cDNA using random hexamers and murine leukemia virus reverse transcriptase. With the cDNA real time PCR was performed with a SYBR green supermix with HSPA1A as a primer. The relative mRNA expression was normalized to GAPDH. To calculate the fold changed  $2^{-\Delta\Delta Ct}$  method (Livak & Schmittgen, 2001) was used and the results show mean fold induction of averaged Ct values.

Figure 25 shows enhancement in HSPA1A expression later in the observed period of time, strongest after 3 hours to 6 hours. Hence, for further experiments, a longer incubation of 4,5 hours was implemented.

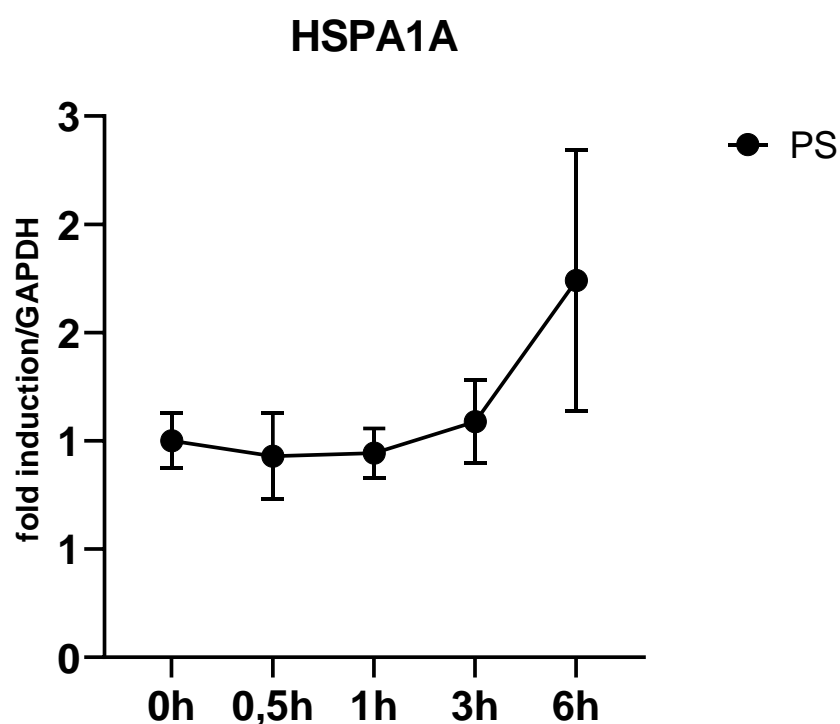


Figure 25 Real time PCR analysis for HSPA1A with 50 µg/ml PS in HEK-293 cells

### 5.2.4 Real time PCR analysis for microfractions 1-35

The large-scale extract of *P. santalinus* was further fractioned. The fractions and micro fractions were obtained by using a recently developed biochemometric approach called ELINA (Eliciting Nature's Activities), which enables the possibility to isolate targeted bioactive compounds. Ptak (2021) provides a detailed description of the fractionation procedure in her diploma thesis. 4 fractions were analyzed. Experiments of former diploma student Ieva R. showed the most promising results for fraction 3. Thus, fraction 3 was additionally fractioned into microfractions. 35 microfractions as well as fraction 3 were examined in a real time PCR analysis for their potential HSPA1A expression. The experiment was conducted in triplets. In 12 well plates cells grew for two days. Afterwards, the cells were treated with 50 µg/ml FR3 and 20 µg/ml for each microfraction. The incubation time was 4,5 hours. The mRNA was extracted using the Qiagen RNeasy Mini Kit and 1 µg mRNA was reverse transcribed into cDNA. Subsequently, with the cDNA, real time PCR was performed with HSPA1A as the primer. Fraction 3 induced HSPA1A expression and was used as a positive control. Microfraction 9,10,11 and 12 also showed increased expression. The same was detected for microfraction 18, 19 and 20. The highest enhancement in expression was observed for microfraction 21. Microfractions 24 and upwards did not show any amplification (figure 26,27 and 28).

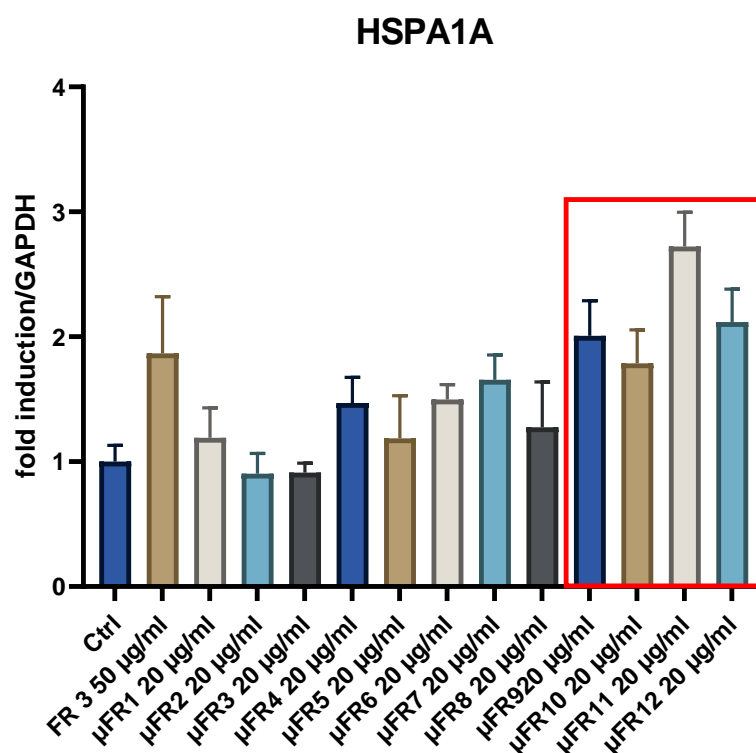


Figure 26 Real time PCR analysis for HSPA1A with 20 µg/ml microfractions 12 – 24



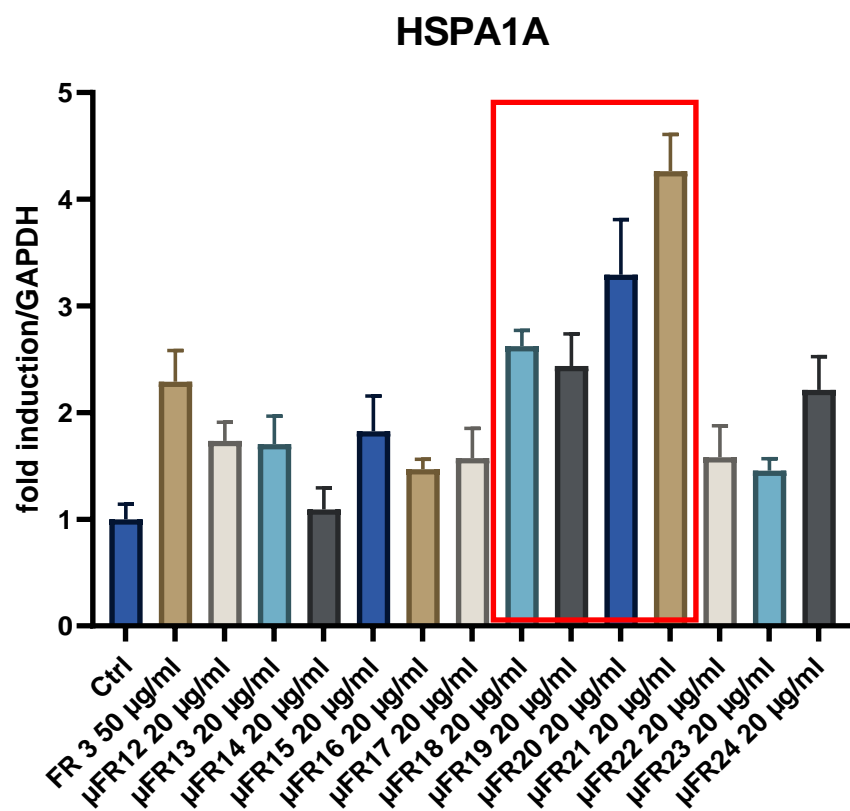


Figure 27 Real time PCR analysis for HSPA1A with 20 µg/ml microfractions 12 - 24

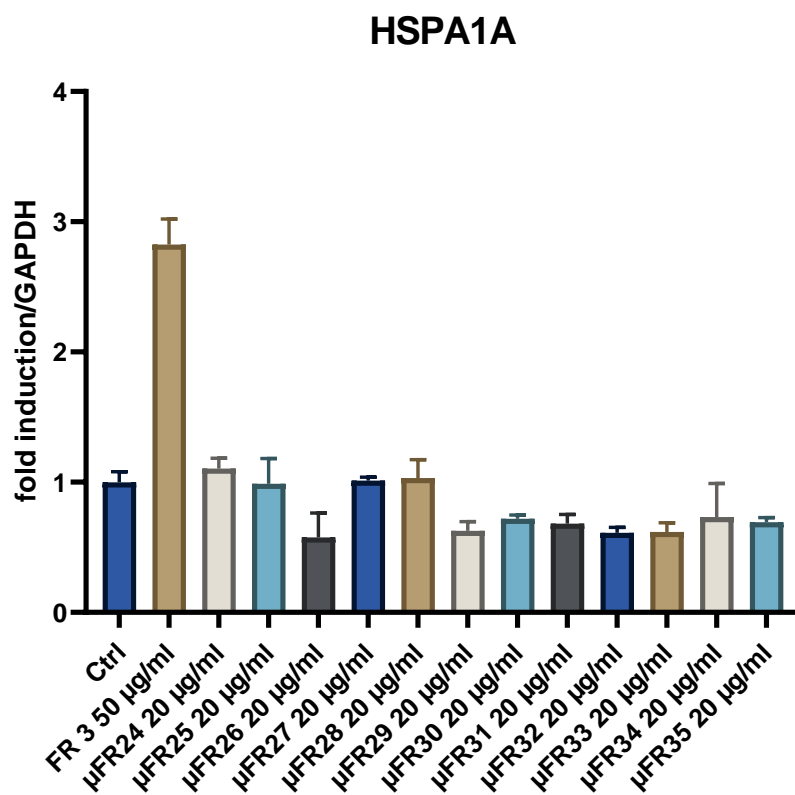


Figure 28 Real time PCR analysis for HSPA1A with 20 µg/ml microfractions 24 - 35

## 6. Conclusion

*P. santalinus* is a valuable medical plant, that is traditionally widely used, especially in Ayurveda, an Indian system of traditional medicine. The heartwood of sandalwood is used externally for the treatment of several maladies, including inflammation, skin diseases or wound healing (Bulle et al., 2016). Despite its longstanding traditional use, only few *in vitro* and *in vivo* studies focusing on its pharmacological activities including anti-inflammatory or antioxidant have been performed (Dahat et al. 2021; Bulle et al. 2016). These studies demonstrated that *P. santalinus* is a valuable, interesting medical plant and further research, focusing on its bioactivity and mode of action is crucial. Thus, experiments based on these characteristics were conducted.

Previous studies of plant-based drugs that are traditionally used for the treatment of inflammation, often show anti-inflammatory activity through NF $\kappa$ B inhibition (Zwirschmayr et al., 2020; Lammel et al., 2020; Seigner et al 2019). This might also be the case for sandalwood. In order to investigate the potential anti-inflammatory activity, real-time PCR analyses were performed. Endothelial cells were used as the *in vitro* study model, due to their key role in the inflammatory response. Prior studies by diploma student Rudžionytė I. focused on PS inhibition in IL-1 stimulated endothelial cells. Considering that PS acts at least partially through NF $\kappa$ B inhibition, further studies, investigating whether PS also inhibits LPS- and TNF-stimulated gene expression, were performed. TNF and LPS signaling pathways differ in the initial stages, but converge at the IKK complex, leading to NF $\kappa$ B (Mercurio et al., 1997). First of all, dose response studies with different concentrations of the two proinflammatory genes provided two suitable concentrations for EC stimulation with 500 ng/ml for LPS and 2,5 ng/ml for TNF. Kinetic analysis of selected PS regulated genes display the progressions of gene-expression over a defined period of time. For LPS, the inhibition was less pronounced over the observed period, as it evokes a slower response compared to TNF. The results displayed that PS downregulates a number of proinflammatory genes. The two genes mostly effected were chemokine CX3CL-1 and TRAF1. As a chemokine, CX3CL1 is responsible for the recruitment of inflammatory cells at the site of inflammation. TRAF1 binds directly to IKK2 and acts as a feedback loop for TNF and LPS signaling pathway (Sughra et al., 2019; Abdul-Sater et al., 2018). The inhibition through PS might prevent the amplification. Further inducible genes downregulated through PS were VCAM-1, a cell adhesion molecule, that regulates

inflammation-associated vascular adhesion and leucocytes migration at inflamed sites (Kong et al., 2018), and PLA2, which is involved in several biological processes including angiogenesis and promotion of vascular permeability (Park et al., 2021). Another noteworthy gene was GM-CSF or CSF2, it is a cytokine that plays a key role in proinflammatory processes by recruiting myeloid cells and enhancing their activation and survival. (Ushach & Zlotnik, 2016). Important to mention is also the downregulation of IRF1, a nuclear factor responsible for the transcription of interferon  $\beta$  (Feng et al., 2021). IRF1 cooperates with NF $\kappa$ B and induces the transcription of VCAM-1 in the inflammatory process (Neish et al., 1995).

Oppositely, various genes were also upregulated by PS. These including NR4A1/2/3 a set of nuclear hormone receptors, all known to play a relevant role in the function of inflammatory cells (Martínez-González et al., 2021) as well as the transcription factor BHLHE40 and the zinc finger protein ZFP36. ZFP36 exhibits anti-inflammatory activity by destabilizing mRNAs of cytokines (Galloway et al., 2016). BHLH is an essential regulator of immunity during inflammatory conditions (Cook et al., 2020). Notably, all of these transcription factors are known to crosstalk with NF $\kappa$ B, a number of PS inducible genes are even able to fully inhibit NF $\kappa$ B or have other functions on EC. (Schichl et al., 2009). As a whole, the tested PS sensitive genes, all exert different functions in the inflammatory process, suggesting that PS mostly acts in an inhibitory matter against inflammatory processes, but might also promote some inflammatory reactions.

Furthermore, heat shock protein HSPA1A was upregulated through PS, independent of proinflammatory stimulation. Thrakl (2019) described promising life extending results for *P.santalinus*. Due to the fact, that studies were able to correlate increased expression of HSPA1A to longevity (de Toda & de la Fuente, 2015), the upregulation of this gene through PS might also be connected to the possible life-extending effect of sandalwood. Moreover, HSPA1A also shows protection against harmful effects of oxidative stress and modulates the inflammatory status (de Toda & de la Fuente, 2015), which could be linked to the antioxidative and anti-inflammatory effects of *P.santalinus*. PS was further fractionized into microfractions, which were also screened for HSPA1A expression. Microfraction 9-12 and 18-20 induced HSPA1A expression. The highest enhancement in expression was observed for microfraction 21. Further studies will aim at the isolation of the responsible compound(s).

## 7. Materials and Methods

### 7.1 Preparation of *P. santalinus* extract and fractions

The large-scale extract of *P. santalinus* and its fractions were prepared at the Department of Pharmacognosy at University of Vienna. Thrakl (2019) provides a detailed description of the extraction and Ptak (2021) of the fractionation in their diploma theses.

### 7.2 Cell culture-HUVEC

For real time PCR experiments human endothelial cells were used, that were directly isolated from umbilical cords and used up until passage 5.

#### 7.2.1 HUVEC isolation from umbilical cords

##### 1. Preparations, Materials and Reagents

- umbilical cords were obtained from the Department of Obstetrics and Gynecology at Vienna General Hospital, Medical University of Vienna. The Ethics Commission of the Medical University of Vienna approved the use of umbilical cords for HUVEC isolation and written informed consent was obtained from the parents.
- sterile materials: syringes (25, 50 ml), syringe attachment filter (EASYstrainer 40 µm), compresses, scissor, cannulas with blunt needles, strings, metal plate, beakers (100 ml, 500 ml), pipettes (10 ml, 25 ml) T25 tissue culture flasks (coated with fibronectin), falcon tubes (15 ml)
- Reagents: 0,1 % Collagenase 1 (80 mg in 80 ml Phosphate buffered saline (PBS)), PBS, 0,05% Trypsin-EDTA (Thermo Fisher Scientific)  
M199 media (Lonza) supplemented with 2 mM -glutamine (Sigma), penicillin (100 units/ml), streptomycin (100 mg/ml), heparin (5 units/ml), 20 % FCS (fetal calf serum, Sigma) and 25 mg/ml ECGS (endothelial cell growth supplement, Promocell)

## 2. Endothelial cell isolation procedure

The isolation was determined under sterile conditions under the laminar air flow hood. The umbilical cord has two arteries and one vein. The vein has a more flexible wall and a larger diameter compared to the arteries (Marin et al., 2001).

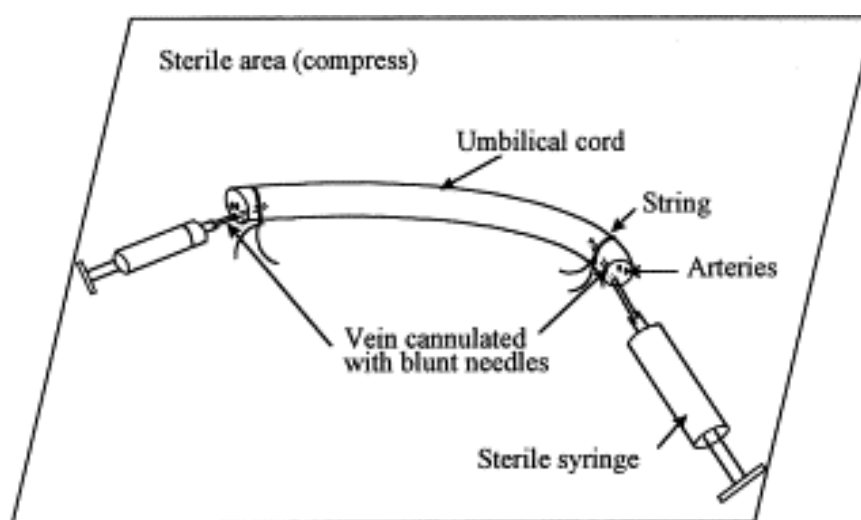


Figure 29 cannulation of the umbilical vein with sterile blunt needles

With sterile blunt needles the umbilical vein was cannulated. The needles were therefore fixed by clamping the cord over the needles using strings. In order to wash out the blood, the vein was then perfused with PBS using a 50 ml syringe. The washing step was continued until the fluid running through became clear. Afterwards, the vein was filled with collagenase 0,1% by using a 25 ml syringe. The cords were placed in an incubator at 37 °C, 5% CO<sub>2</sub>, for 7 minutes. After incubation, the fluid inside the cords was discharged respectively into 15 ml falcon tubes (squeezing of the cord helped with cell detachment). Each tube should contain the same amount of liquid. Therefore the differences were filled up with PBS. The cells were centrifuged at room temperature for 5 minutes relative centrifugal force (RCF) 300. The medium was discarded, and cells were resuspended in 5 ml M199 media (+ supplements). The cells were transferred in prior prepared T25 cell culture flasks (coated with fibronectin) and incubated overnight.

### **7.2.2 HUVEC passaging**

After 24 h incubation, the media was changed and after growing for another 24 h (or longer, until cells reached 80-90 % confluence), the cells were transferred into prior prepared T75 flasks, coated with 1% gelatin. Therefore, media was discarded, and confluent cells were washed twice with 1-2 ml PBS, then 2 ml 0,05% Trypsin - Ethylenediamine tetraacetic acid (EDTA) was added, and cells were incubated for about 5 minutes at 37 °C, until all cells were detached. In order to stop cell detachment, 12 -14 ml prewarmed media was added. After repeated pipette aspiration, cell suspension was transferred to the T75 flask and carefully distributed by moving the flask in each direction. Cells were incubated for about 2 days (depending on cell growth). The doubling time for HUVEC varies from 17 to 24 hours from first to fourth passage (Marin et al., 2001). Cells were used up until passage 5.

### **7.2.3 Real-time PCR analysis**

#### Plating cells

Before cells could be plated, it was important to check if they were healthy and growing as expected. This was done every day whilst incubation. The health of the cells can be determined by their shape, which is rather elongated in the state of confluence and their attachment to the surface. The color of the media also provides an indicator for the state of health. It should be pinky orange (Abcam, 2021). After checking and reaching a confluency of 80% - 90 %, cells were plated in 12 well plates. Therefore, the media was discarded, cells were washed twice with 3-4 ml of PBS and 2-3 ml of 0,05 % Trypsin-EDTA was added for trypsinization. Cells were incubated for about 5 minutes at 37 °C, until all cells were detached. Counting was used to ascertain the right number of cells for plating. The cell suspension was diluted with media and thoroughly mixed through pipetting. A sample of about 1 ml was taken out and cells were counted using a hemocytometer (Neubauer chamber).

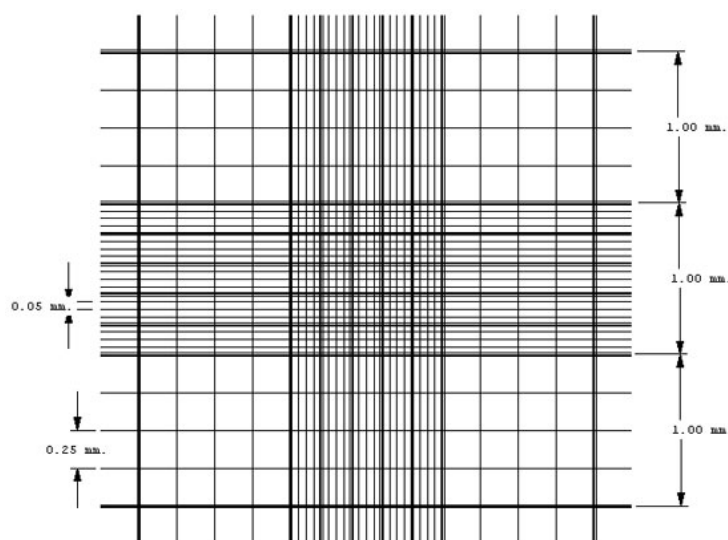


Figure 30 Neubauer chamber

The area of one square in the Neubauer chamber equals  $0,01 \text{ cm}^2$ , while the depth of the chamber equals  $0,01 \text{ cm}$ . Giving this, the volume of one square equals  $0,0001 \text{ ml}$ . By counting the number of cells in the squares and dividing the total number of cells by volume, the concentration of cells per ml can be obtained. (Proteintech, 2021)

The seeding density for a 12 well plate is about  $0,1 \times 10^{12} \text{ cells/ml}$ . The following formula was used for calculating the amount of cell suspension needed and the amount of media needed for diluting the cell suspension.

$$c1 \times v1 = c2 \times v2$$

After calculation and dilution, cells were plated in a 12 well plate, that was precoated with 1% gelatin. This was conducted by adding 1 ml of the diluted cell suspension to each well and carefully contributing the cells through moving the plate in each direction. Cells were incubated again at  $37^\circ \text{C}$  and grown for about two days until post confluency.

### Experiment procedure

The experiments were executed when cells were at post confluency. Depending upon experimental requirements, cells were pretreated with 50 µg/ml PS or with 25 µg/ml FR3 or 20 µg/ml µFR and stimulated with either 2,5 ng/ml TNF or 500 ng/ml LPS. Experiments were conducted in triplets and cells, left untreated, served as control. For stimulation, no new media was used. The media, that was already in the 12 well plates, was provided with the correct amount of TNF/LPS, enabling the media, that was added back on the cells, to contain 2,5 ng/ml TNF or 500 ng/ml LPS. If cells were pretreated with sandalwood, prior to stimulation, the media was diluted with PS/FR3/µFR to the correct concentrations and afterwards, cells were incubated for 30 minutes at 37 °C. After pretreatment and stimulation, cells were incubated for a certain period of time. Incubation time varied upon experimental requirements.

### mRNA extraction

After cell treatment and incubation time, media was discarded from the cells, and they were washed twice with PBS. Two different kits, the PeqGold Total RNA Isolation Kit by VWR international and the RNeasy Mini Kit by Qiagen were used according to the manufacturer's instructions to extract the mRNA.

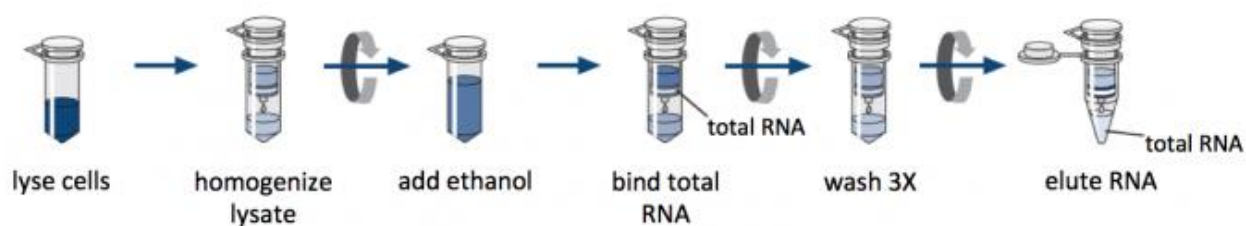


Figure 31 mRNA extraction procedure



Both kits use the same strategy for mRNA extraction. The cells can be lysed directly in the 12 well plate with the provided lyse buffer. Afterwards, they are homogenized through uploading on a homogenizer column and centrifugation at maximum speed. The flow through is diluted with 70 % ethanol, loaded on the binding column and again centrifuged. The flow through can be discarded and the binding column is washed three times with the provided wash buffers. The gained mRNA can then easily be eluted using the provided RNase free water.

### cDNA synthesis

1 µg of the mRNA was reverse transcribed into cDNA. First of all, in order to ascertain the exact amount of respectively obtained mRNA, UV-VIS spectroscopy was performed with the NANODROP 2000c by Thermo Scientific. Thereby the light absorption at 260 nm was measured and with a specific factor (40) the concentration of RNA calculated. To exclude contamination, light absorption at 280 and 230 was also measured. Knowing the exact concentration, 1000 ng of RNA were then used for cDNA synthesis. RNA was diluted using deionized, diethylpyrocarbonate (DEPC)-treated water. The RNA samples were stored on ice, while the experiment was prepared.

A mastermix was prepared for x-reactions containing:

- 4 µg 5x Reverse Transcriptase (RT) buffer (Fisher scientific)
- 2 µg MgCl<sub>2</sub> (50 mM) (Fermentas)
- 1 µg random hexamers (Fisher scientific)
- 0,25 µg murine leukemia virus reverse transcriptase (Fisher scientific)
- 2,5 µg deoxynucleotide triphosphates (dNTPs 25 mM) (Fermentas)

In a 96 well plate 20 µl of the final reaction solution (diluted RNA + mastermix) was added in each well. The mRNA was then reversed-transcribed into cDNA using the thermocycler GeneAmp PCR System 2700 by Applied Biosystems.

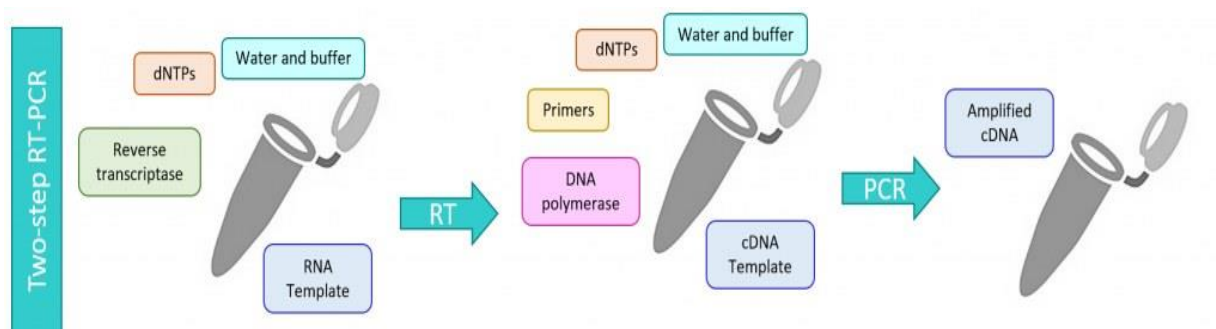


Figure 32 The two steps of mRNA reversed transcription into cDNA and polymerase chain reaction for cDNA amplification

### Amplification of cDNA

The cDNA was now diluted with 80 µl DEPC-treated water and 2 µl were added to a 96 well PCR plate. During the entire procedure, the samples were stored on ice and the PCR plate was cooled by using a cool block. For the PCR analysis specific primers, depending on each experiment, were used, that were designed with the software “Primer 3” as described in Natalia et al. (submitted 2021). A reaction solution with 0,5 µl of forward and reverse primers, 4 µl of SsoAdvanced Universal SYBR Green Supermix (BioRad) and 3 µl of DEPC treated water was prepared and added into the with cDNA filled wells. Real time PCR was performed using the StepOnePlus instrument (Applied Biosystems). For the results, glyceraldehyde-3-phosphate dehydrogenase (GAPDH), a glycolytic enzyme, catalyzing the conversion of glyceraldehyde-3-phosphate (Zhang et al., 2015) was used to normalize relative mRNA expression. The  $2^{-\Delta\Delta C_t}$  method (Livak & Schmittgen, 2001) was utilized to calculate the fold changes in mRNA expression. The results were evaluated in triplets and show the mean fold induction of averaged  $C_t$ -values.

## **7.3 Cell-culture HEK-293 cell-line**

HEK-293 cells were used for real time PCR analysis and for a cytotoxicity assay.

### **7.3.1 Thawing of HEK-293 cells**

HEK-293 cells were stored at liquid nitrogen. Cells were thawed for the execution of the experiments. This process must be performed quickly and under the laminar air flow to establish sterile conditions. Before thawing the cells, media was prepared using Dulbecco's Modified Eagle's Limiting Media (DMEM), that was supplemented with 20 % FCS, 2mM L-glutamine, penicillin (100 units/ml) and streptomycin (100 µg/ml). In order to thaw the cells, the vial of frozen cells was removed from liquid nitrogen and heated in a 37 °C water bath. Just before the cells were completely thawed, the outside of the vial was disinfected, put under the laminar airflow and 1 ml of the prior prepared media was added in. Through repeated pipetting, cells and media were mixed through thoroughly, the suspension was transferred to a 15 ml falcon tube and centrifuged for 5 minutes, RCF 300 at 4 °C. Afterwards, the media was discarded, and cells were resuspended in 5 ml fresh DMEM (+supplements). The cell suspension was transferred into a T25 cell culture flask and incubated at 37 °C overnight.

### **7.3.2 HEK-293 passaging**

After overnight incubation, cells were checked for health and cell growth, media was changed, and cells were again incubated and grown up until 80-90 % confluency. Cells were then transferred into a T75 cell culture flask. Therefore, media was discarded, cells were washed once with PBS and 1 ml trypsin was added for trypsinization. After incubation of 2-3 minutes, 12-15 ml of media was added into the cell culture flask, through pipetting the cell suspension was mixed thoroughly and transferred into the T75 flask. Cells were contributed carefully by moving the flask in each direction and again incubated at 37 °C for about 2 days until cells reached 80-90% confluence.

### 7.3.3 Freezing of HEK-293 cells

After trypsinization and resuspension with media, 1 ml of the cell suspension was transferred into a 15 ml falcon tube for freezing. The rest of the cell suspension was transferred into the T75 flask. Cells were frozen for possible future experiments. For this purpose, cells were centrifuged at 4°C, RCF 300 for 5 minutes. The media was discarded, and cells were resuspended in 1 ml ice cold 10% dimethyl sulfoxide (DMSO) media (10% DMSO, 90% DMEM + supplements). The cell suspension was then transferred into 1,5 ml cryovials. First it was slowly frozen at -80 °C for 24 h and afterwards stored at liquid nitrogen.

### 7.3.4 Cell Titer-Blue Cell Viability assay

The “Cell Titer-Blue Cell Viability Assay” by Promega was performed to investigate the potential toxicity of *P. Santalinus* on HEK-293 cells.

#### Plating cells

For the experiment cells were plated in 96-well plates. The plating method is described in 7.2.3 “Real-time PCR analysis” under “Plating cells”. HEK-293 cells and HUVEC were plated following the same procedure. The only difference was that for HEK-293 cells no prior coating of the flasks and plates with 1% gelatin was necessary and the seeding density for 96-well plates is  $0,01 \times 10^6$ . After calculation and dilution, 200 µl of the prepared cell suspension was added to each well and the cells were contributed carefully. Cells were incubated at 37°C for about 2 days or until cells reached post confluency.

### Experiment procedure

The experiment was conducted in triplets and followed the manufacturer's recommendations. When cells reached post confluency they were treated with different concentrations of PS (200/100/50/25/12,5/6,25/3,125 µg/ml). 4 µl of a lysis buffer was used as toxicity control. For detailed description of cell treatment see 7.2.3 "Real-time PCR analysis" under "Experiment procedure". Treated cells were incubated at 37°C for 6 hours. 20 µl of the provided cell titer blue reagents was added to each well and cells were incubated for 2 more hours. The reaction was stopped by adding 3% SDS to the wells. Fluorescence was read at 520/590 nm using the Synergy H4 Hybrid Reader by BioTek. For the evaluation of the data, the average fluorescence values of the culture medium background were subtracted from all fluorescence values of experimental wells. Cell viability was specified in percent.

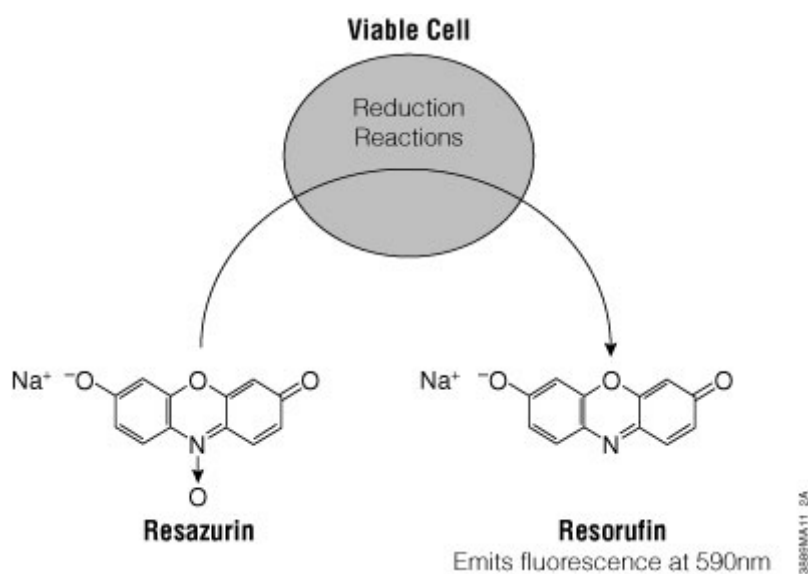


Figure 33 Viable cells reduce Resazurin to Resorufin

The viability assay uses resazurin as an indicator, viable cells dispose the possibility to reduce resazurin to resorufin, which is highly fluorescent and can be measured at 590 nm.

### 7.3.5 Real-time PCR analysis in HEK-293 cells

Real-time PCR analysis was also performed with HEK-293 cells. Therefore, cells were plated in 12 well plates and grown until post confluency. For a detailed description see 7.2.3 “Real-time PCR analysis” under “Plating cells” and “Experiment procedure”. Depending on the experiment, cells were treated with 50 µg/ml PS, 25 µg/ml FR3 or 20 µg/ml µFR of *P. santalinus*. No prior stimulation of the cells was needed. Cells were incubated for a certain period of time. Incubation time varied upon experimental requirements. Afterwards, the media was discarded, and cells were washed once with PBS. In order to preserve the cells and stabilize the RNA, a solution of 1:5 of PBS and RNAlater (Sigma) was prepared and 400 µl was added to each well. The plates were stored at -20°C until mRNA extraction. The extraction was conducted by using the RNeasy Mini Kit by Qiagen according to the manufacturer's instructions. 1 µg of the mRNA was reverse-transcribed into cDNA using murine leukemia virus reverse transcriptase and random hexamers (see 7.2.3 “Real-time PCR analysis” under “cDNA synthesis”). Real time PCR was performed with HSPA1A as primer, details can be found at 7.2.3 under “cDNA amplification”.

## 7.4 Instruments and Products

Table 1 Instruments and their description and supplier

<b>Instruments</b>	<b>Description/Supplier</b>
centrifuge	5145R Eppendorf 1-16KS Sigma
microscope	Nikon TMS
Thermocycler	GeneAmp PCR System 2700, Applied Biosystem
Laminar Air Flow	MSC-Advantage, ThermoScientific
incubator	HERACELL 150i, ThermoScientific
Real-Time PCR system	StepOnePlus, Applied Biosystem
spectrophotometer	Nanodrop 2000c, ThermoScientific
microplate reader	Synergy H4, BioTek
mRNA extraction kits	RNeasy Plus Mini Kit, Qiagen RNeasy Plus Micro Kit, Qiagen PeqGold Total RNA Isolation Kit, VWR

## 8. Acknowledgments

First, I would like to thank Prof. Dr. **Judith M. Rollinger** for the opportunity to write my diploma thesis at the department of Pharmacognosy in cooperation with the department of Vascular Biology and Thrombosis Research at the medical university of Vienna. Thank you for the effort to make this cooperation possible for me. Although I did most of my work at the medical university, Prof. Rollinger always made sure, that I also felt welcome and supported at the Pharmacognosy department. I also want to thank **Julia Zwirchmayr**, who always helped me with my pharmacognostic questions.

I would like to thank Prof. Dr. **Rainer de Martin** for the opportunity to work at the medical university of Vienna as his diploma student. Prof. de Martin patiently explained everything to me, his door was always open for any questions and guidance. He always took the time to discuss my results with me in detail. Whenever he chose to work from home, he always made sure to be reachable and answered every e-mail as soon as possible.

A huge thanks to the whole **team of the vascular biology group** for the welcoming atmosphere despite Covid-19. I would like to especially thank **Ieva** for patiently teaching me how to work with cells. She always had an open ear for my questions and also helped me with analyzing my data. She even stayed with me in the lab until late at night to help me with my experiments. I also want to thank **Lucas** for his advice and for the necessary lunch breaks.

Finally, my deepest gratitude to my **family and friends**, especially my parents and siblings as well as my roommates (my second family), for your support, patience, encouragement and love through the years-Thanks a lot!



## 9. References

### Articles

de Martin R. (2019) Endothelial Cells: Function and Dysfunction. In M. Geiger, *Learning Materials in Biosciences*, S. 82-95.

Proteintech (2021) Cell Culture Protocol. In *The Complete Guide to Cell Culture*, S. 18-23

Promega (2021) General Considerations, Protocol. In *CellTiter-Blue Cell Viability Assay* S. 6-10

Abcam (2021) Cell Culture Plating. In *Toxin neutralization assay cell preparation/ plating* S.1-2

### Diploma theses

Ptak (2021) "Isolation and Characterization of bioactive constituents from *Pterocarpus santalinus* affecting the healthspan of *Caenorhabditis elegans*", Diploma Thesis, Univ. Wien.

Thrakl A. (2019) "Unravelling the lifespan increasing potential of *Pterocarpus santalinus* in a phenotypic *Caenorhabditis elegans* lifespan assay", Diploma Thesis, Univ. Wien.

### Websites

Images:

[http://www.sailasyahitechnursery.com/red\\_sandalwood.html](http://www.sailasyahitechnursery.com/red_sandalwood.html)

assessed September 2021

<http://indiasendangered.com/red-alert-for-red-sanders-the-rare-red-coloured-timber/>

assessed September 2021

<https://www.ahajournals.org/doi/full/10.1161/01.ATV.20.11.e83>

assessed October 2021

<https://innoprot.com/product/red-fluorescent-hek-293-cell-line/>

assessed October 2021

[https://www.sciencellonline.com/media/catalog/product/cache/1/image/a6f8fb4f61eb724c ff40f184d1fbcab0/8/0/8000\\_1.jpg](https://www.sciencellonline.com/media/catalog/product/cache/1/image/a6f8fb4f61eb724c ff40f184d1fbcab0/8/0/8000_1.jpg)

assessed October 2021

<https://www.sciencedirect.com/science/article/pii/S0022175901004082>

assessed November 2021

<https://laboratoryinfo.com/wp-content/uploads/2016/05/63511.jpg>

assessed November 2021

[http://measurebiology.org/w/images/thumb/0/02/Sp17\\_20.109\\_M2D3\\_RNA\\_purification.png/750px-Sp17\\_20.109\\_M2D3\\_RNA\\_purification.png](http://measurebiology.org/w/images/thumb/0/02/Sp17_20.109_M2D3_RNA_purification.png/750px-Sp17_20.109_M2D3_RNA_purification.png)

assessed November 2021

<https://www.anawa.ch/it/acquisto/cat-two-step-rt-qpcr-mixes-sybr-green-3551.html>

assessed November 2021

[https://france.promega.com/resources/guides/cell-biology/cell-viability/~Media/Images/Resources/PAGuide/3889MA11\\_2A.ashx](https://france.promega.com/resources/guides/cell-biology/cell-viability/~Media/Images/Resources/PAGuide/3889MA11_2A.ashx)

assessed November 2021

## Papers

- Abdul-Sater A., Edilova M., Clouthier D., Mbanwi A., Kremmer E., Watts T. (2017) The signaling adaptor TRAF1 negatively regulates Toll-like receptor signaling and this underlies its role in rheumatic disease. *Nat Immunol* 18(1), 26-35.
- Bulle S., Reddyvari H., Nallanchakravarthula V., Vaddi D. R. (2016) Therapeutic Potential of *Pterocarpus santalinus* L.: An Update. *Pharmacogn Rev* 10, 43-49.
- Cook M., Jarjour N., Lin C.-C., Edelson, B. (2020) Transcription Factor Bhlhe40 in Immunity and Autoimmunity. *Trends Immunol.* 41(11), 1023-1036.
- Dahat Y., Saha P., Mathew J., Chaudhary S., Srivastava A., Kumar D. (2021) Traditional uses, phytochemistry and pharmacological attributes of *Pterocarpus santalinus* and future directiones: A review. *J. Ethnopharmacol* 276.
- de Martin R., Hoeth M., Hofer-Warbinek R. A., Schmid J. (2000) The Transcription of NFκB and the Regulation of Vascular Cell Function. *Atheroscler Thromb Vasc. Biol.* 20, 83-88.
- de Toda I. M., Vida C., Ortega E., de La Fuente M. (2016) Hsp70 basal levels, a tissue marker of the rate of aging and longevity in mice . *Exp Gerontol* 84, 21-28.
- de Toda M., de La Fuente, M. (2015) The role of Hsp70 in oxi-inflamm-aging and its use as a potential biomarker of lifespan. *Biogerontology* 16(6), 709-21.
- Edilova M., Abdul-Sater A., Watts T. (2018) TRAF1 Signaling in Human Health and Disease . *Front. Immunol.*
- Egger B., van Giesen L., Moraru M., Sprecher S. (2013) In vitro imaging of primary neural cell culture from *Drosophila*. *Nat Protoc.* 8(5), 958-65.
- Feng H., Zhang Y.-B., Gui J.-F., Lemon S., Yamane D. (2021) Interferon regulatory factor 1 (IRF1) and anti-pathogen innate immune responses. *PLoS Pathog* 17(1).
- Galloway A., Saveliev A., Lukasiak S., Hodson D., Bolland D., Ballmano K., Ahlfors H., Monzón-Casanova E., Mannurita S.C., Bell L.S., Andrews S., Díaz-Muñoz M.D., Cook S.J., Corcoran A., Turner, M. (2016) RNA binding proteins ZFP36L1 and ZFP36L2 promote cell quiescence. *Science* 352, 453-459.
- Han Y.-F., Cao, G.-W. (2021) Role of nuclear receptor NR4A2 in gastrointestinal inflammation and cancers. *World J Gastroenterol* 18(47), 6868-6873.
- Jones B., Beamer M., Ahmed S. (2010) Fractalkine/CX3CL1: A Potential New Target for Inflammatory Diseases. *Mol Interv.* 10(5), 263-270.
- Kankanange K., Charana W. B., Siripala S., Min-Ho Y. (2011) *Pterocarpus Santalinus* Linn. f. (Rath hadnun): A Review of Its Botany, Uses, Phytochemistry and Pharmacology. *J. Korean Soc. Appl. Biol. Chem.* 54(4), S. 495-500.
- Kong D.-H., Kim Y. K., Kim M. R., Jang J. H., Lee S. (2018) Emerging Roles of Vascular Cell Adhesion Molecule-1 (VCAM-1) in Immunological Disorders and Cancer. *Int J Mol Sci.* 19(4), 1057.

- Lammel C., Zwirchmayr J., Seigner J., Rollinger J., de Martin, R. (2020) Peucedanum ostruthium Inhibits E-Selectin and VCAM-1 Expression in Endothelial Cells through Interference with NF- $\kappa$ B Signaling. *Biomolecules* 10, 1215.
- Lanig H., Reisen F., Whitley D., Schneider G., Banting L., Clark T. (2015) In Silico Adoption of an Orphan Nuclear Receptor NR4A1. *PLoS One* 10(8).
- Lin Y.-C., Boone M., Meuris L., Lemmens I., Van Roy N., Soete A., Reumers J., Moisse M., Plaisance S., Drmanac R., Chen J., Speleman F., Lambrechts D., Van de Peer Y., Tavernier J., Callewaert N. (2014) Genome dynamics of the human embryonic kidney 293 lineage in response to cell biology manipulations. *Nat Commun* 5, 4767.
- Livak K. J., Schmittgen T. D., (2001) Analysis of relative gene expression data using real-time quantitative PCR and the 2(-Delta Delta C(T)) Method. *Methods* 25, 402-408.
- Martínez-González J., Cañes L., Alonso J., Ballester-Servera C., Rodríguez-Sinovas A., Corrales I., Rodríguez C. (2021) NR4A3: A Key Nuclear Receptor in Vascular Biology, Cardiovascular Remodeling, and Beyond. *Int. J. Mol. Sci.* 22(21).
- Medina-Leyte D., Domínguez-Pérez M., Mercado I., Villarreal-Molina M., Jacobo-Albavera L. (2020) Use of Human Umbilical Vein Endothelial Cells (HUVEC) as a Model to Study Cardiovascular Disease: A Review. *Appl.Sci.* 10(3).
- Mercurio F., Zhu H., Murray B., Shevchenko A., Bennett B., Li J., Young D.B., Barbosa M., Mann M., Manning A., Rao A. (1997) IKK-1 And IKK-2: Cytokine-Activated I $\kappa$ B. *SCIENCE* 278, 860-866.
- Natalia P., Zwirchmayr J., Rudžionytė I., Pulsinger A., Breuss J., Uhrin P., Rollinger J. M., de Martin R. Pterocarpus santalinus inhibits selectively a subset of pro-inflammatory genes in interleukin-1 stimulated endothelial cells; submitted 11/2021, *Front. Pharmacol.*
- Neish A., Read A., Thanos D., Pine R., Maniatis T., Collins T. (1995) Endothelial interferon regulatory factor 1 cooperates with NF-kappa B as a transcriptional activator of vascular cell adhesion molecule 1. *Mol Cell Biol.* 15(5), 2558-69.
- Park J. E., Eunmi K., Lee D.-W., Park T. K., Kim M. S., Jang S. Y., Ahn J., Park K.B., Kim K.-H., Park H.-C., Ki C.-S., Kim D.-K. (2021) Identification of de novo EP300 and PLAU variants in a patient with Rubinstein–Taybi syndrome-related arterial vasculopathy and skeletal anomaly. *Sci Rep* 11, 15931.
- Sankaran K. R., Ganjari M. S., Oruganti L., Chippada A. R., Meriga B. (2021) A bioactive fraction of Pterocarpus santalinus inhibits adipogenesis and inflammation in 3T3-L1cells via modulation of PPAR- $\gamma$ /SREBP-1c and TNF- $\alpha$ /IL-6. *Biotech* 3.
- Schichl Y., Resch U., Hofer-Warbinek R., de Martin R. (2009) Tristetraprolin impairs NF- $\kappa$ B/p65 nuclear translocation. *J. Biol. Chem.*, 284.
- Seigner J., Junker-Samek M., Plaza A., D'Urso G., Masullo M., Piacente S., Holper-Schichl Y. M., de Martin R. (2019) A Symphytum officinale Root Extract Exerts Anti-

- inflammatory Properties by Affecting Two Distinct Steps of NFkB Signaling. *Front. Pharmacol.* 10, 1-12.
- Su R., Jin X., Li H., Huang L., Li, Z. (2020) The mechanisms of PM2.5 and its main components penetrate into HUVEC cells and effects on cell organelles. *Chemosphere* 241.
- Sughra K., Birbach A., de Martin R. (2010) Interaction of the TNFR-Receptor Associated Factor TRAF1 with I-Kappa B Kinase-2 and TRAF2 Indicates a Regulatory Function for NF-Kappa B Signaling. *PLoS ONE* 5(9), e12683.
- Thomas P., Smart T. (2005) HEK293 cell line: A vehicle for the expression of recombinant proteins. *J. Pharmacol. Toxicol. Methods* 51, 187-200.
- Toliver-Kinsky T., R.Sherwood E. (2004) Mechanisms of the inflammatory response. *Elsevier* 3, 385-405.
- Ushach I., Zlotnik A. (2016) Biological role of granulocyte macrophage colony-stimulating factor (GM-CSF) and macrophage colony-stimulating factor (M-CSF) on cells of the myeloid lineage. *J Leukoc Biol.* 100(3), 481-489.
- Valérie M., Kaplanski G., Grès S., Farnarier C., Bongrand P. (2001) Endothelial cell culture: protocol to obtain and cultivate human umbilical endothelial cells. *J. Immunol. Methods*, 183-190.
- Valerius M.T., Patterson L.T., Feng Y., Potter S.S., (2002) Hoxa 11 is upstream of Integrin  $\alpha 8$  expression in the developing kidney. *PNAS* 99(12), 8090-8095.
- Zhang J.-Y., Zhang F., Hong C.-Q., Giuliano A., Cui X.-J., Zhou G.-J., Zhang G.J., Cui Y.-K. (2015). Critical protein GAPDH and its regulatory mechanisms in cancer cells. *Cancer Biol Med.* 12(1), 10-22.
- Zhao Y., Sun H., Lu J., Li X., Chen X., Tao D., Huang W., Huang B. (2005) Lifespan extension and elevated hsp gene expression in *Drosophila* caused by histone deacetylase inhibitors. *J Exp Biol.* 208, 697-705.
- Zwirschmayr J., Grienke U., Hummelbrunner S., Seigner J., de Martin R., Dirsch V., Rollinger J. (2020). A Biochemometric Approach for the Identification of In Virto Anti-Inflammatory Constituents in Masterwort. *Biomolecules* 10, 679.